Tectonics

RESEARCH ARTICLE
10.1029/2017TC004910

Key Points:
- Structure of the fold-and-trust belt in southwest Taiwan
- Development of a fold-and-thrust belt on the outer continental margin and slope
- Along-strike changes in structure that have a causal relationship with variations in the basal thrust that, in turn, is related to basement

Supporting Information:
- Supporting Information S1
- Table S1
- Figure S1

Correspondence to:
D. Brown,
dbrown@ictja.csic.es

Citation:
Biete, C., Alvarez-Marron, J., Brown, D., & Kuo-Chen, H. (2018). The structure of southwest Taiwan: The development of a fold-and-thrust belt on a margins outer shelf and slope. *Tectonics*, *37*, 1973–1993. https://doi.org/10.1029/2017TC004910

Received 29 NOV 2017
Accepted 18 JUN 2018
Accepted article online 26 JUN 2018
Published online 16 JUL 2018

The Structure of Southwest Taiwan: The Development of a Fold-and-Thrust Belt on a Margins Outer Shelf and Slope

Cristina Biete[1], Joaquina Alvarez-Marron[1], Dennis Brown[1], and Hao Kuo-Chen[2]

[1]Institute of Earth Sciences, Barcelona, Spain, [2]Department of Earth Science, National Central University, Zhongli, Taiwan

Abstract The southwest Taiwan fold-and-thrust belt is forming on the outer shelf and slope of the Eurasian continental margin. It comprises a roughly N-S striking, west verging imbricate thrust system that has been developing since the Late Miocene. Here we present the results of new surface geological mapping from which we construct balanced and restored cross sections and along-strike sections. From these we compile maps of the basal thrust, thrust branch lines and, where possible, stratigraphic cutoffs. To interpret the structure in the subsurface and beneath the basal thrust, we use a *P* wave velocity of 5.2 km/s as a proxy for the top of the Mesozoic basement. We divide the southwest Taiwan fold-and-thrust belt into a number of thrust sheets that form the basis of our description and interpretations. From these data we interpret the 3-D structure of the fold-and-thrust belt and the influence that the structure and morphology of the continental margin is having on its development. We show that there is a significant along-strike change in the structure. This change takes place across a transverse zone that is composed of a suite of structures at the surface. We suggest that this transverse zone has a causal relationship with variations in the geometry of the basal thrust which in turn is related to (possibly fault bounded) basement highs and lows that are inherited from the continental margin.

Plain Language Summary The southwest Taiwan fold-and-thrust belt comprises a roughly N-S striking, west verging imbricate thrust system that has been developing since the Late Miocene. We present the results of new surface geological mapping from which we construct balanced and restored cross sections and along-strike sections. We compile maps of the basal thrust, thrust branch lines, and stratigraphic cutoffs. We divide the southwest Taiwan fold-and-thrust belt into a number of thrust sheets that form the basis of our description and interpretations. From these data we interpret the 3-D structure of the fold-and-thrust belt and the influence that the structure and morphology of the continental margin is having on its development. We show that there is a significant along-strike change in the structure. This change takes place across a transverse zone that is composed of a suite of structures at the surface. We suggest that this transverse zone has a causal relationship with variations in the geometry of the basal thrust which in turn is related to (possibly fault bounded) basement highs and lows inherited from the continental margin.

1. Introduction

In many fossil orogens, the involvement of the shelf or slope of the incoming continental margin, and the reactivation of faults on these parts of the margin, can often be shown to have played an important role in the structural evolution of their fold-and-thrust belts (e.g., Butler et al., 2006; Faulds & Varga, 1998; Flöttmann & James, 1997; Smith, 1999; Zanchi et al., 2006). Nevertheless, from these preserved rock records it is not always straightforward what the initial configuration of the margins morphological and structural architecture were with respect to the developing fold-and-thrust belt, since they may be masked by large translation along thrusts and/or because of dismemberment by subsequent tectonic activity. Despite the difficulties, along-strike changes in the structural architecture of a fold-and-thrust belt are often interpreted to be caused by the reactivation of preexisting faults or changes in sedimentary thickness and facies that were inherited from the continental margin involved, although generally without specifics of where on the margin these came from or what their original architecture was (e.g., Arora et al., 2012; Duncan et al., 2003; Mouthereau et al., 2006; Pérez-Estaún et al., 1997; Thomas, 1985; Turner et al., 2010; Yin, 2006). Therefore, investigating an active orogen in which a continental margin is being deformed can yield important information about how a margins morphology and structure affect not only the structural architecture of a fold-and-thrust belt but also transient features such as seismicity and topography (e.g., Brown et al., 2017).

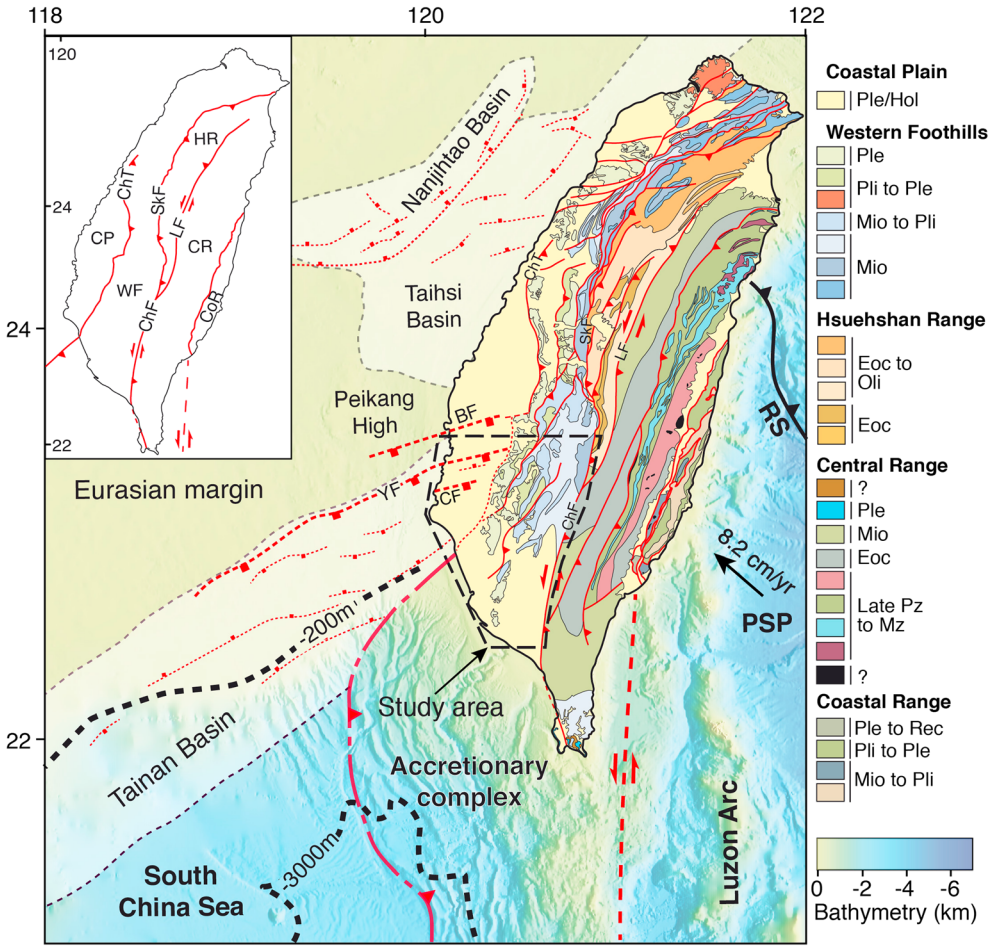

Figure 1. Tectonic setting of the Taiwan arc-continent collision orogen with location of the Taiwan island in relation with the Luzon arc and its accretionary complex, the Ryukyu trench (RS) and major basins of the Eurasian margin. A simplified geological map of the island of Taiwan is shown (after C.-H. Chen et al., 2000), and the main tectonic units are in the inset. The Tainan, Taihsi, and Nanjihtao basins offshore Taiwan include significant extensional structures oriented at a high angle to the structural grain of the orogen. The location of bathymetric contours 200- and 3,000-m depth is shown. The location of the study area is also shown. The convergence vector of 8.3 cm/year between the Philippine Sea Plate and the southern part of the Eurasian Plate is also given. PPS = Philippine Sea Plate; ChT = Changhua thrust; LF = Lishan Fault, SkF = Shuilikeng Fault; ChF = Chauchou Fault; BF = B fault; YF = Yichu fault; CF = Chiali fault. The inset shows the tecto-nostratigraphic units of the Taiwan orogen. CP = coastal plain; WF = western Foothills; HR = Hsuehshan Range; CR = Central Range; CoR = Coastal Range.

Taiwan is a particularly propitious place for carrying out this type of study because the main morphological parts of the margin, including the shelf, the shelf-slope break (defined as the 200-m bathymetry contour), and the hyperextended part of the margin (starting at about the 3,000-m bathymetry contour [e.g., McIntosh et al., 2014]), as well as the extensional fault systems (A. T. Lin et al., 2003; Yang et al., 1991) that make up the structural necking zone (Brown et al., 2017), are all at a high angle to the developing structural grain of the fold-and-thrust belt (Figure 1). Therefore, it is possible to trace these margin features into the fold-and-thrust belt and to readily determine how (or if) they are affecting its structural evolution (e.g., Alvarez-Marron et al., 2014; Brown et al., 2017; Mouthereau et al., 1999, 2002; Suppe, 1986; Yang et al., 2007, 2016). In a number of recent publications (e.g., Alvarez-Marron et al., 2014; Brown et al., 2012, 2017; Camanni et al., 2016), we have explored the effect that the morphology and structure of the Eurasian continental margin is having on the structural evolution of the fold-and-thrust belt of south-central Taiwan. In these publications we proposed that effects of both the morphological (the shelf, the shelf-slope break, the slope) and the structural (the necking zone) parts of the margin can be seen in the Taiwan fold-and-thrust belt as along-strike changes in structure, seismicity, and topography (Brown et al., 2017). In this paper we build on this theme,

Figure 2. Chronostratigraphic correlation chart used in the mapping. It is based on Shea et al. (2003).

presenting the results of new geological mapping of the fold-and-thrust belt in southwest Taiwan (Figure 1), providing a detailed analysis of its structural architecture, how this changes from north to south, and what the suite of structures are that occur along the area of change. We go on to propose how these areas of along-strike structural change can be related to the preexisting structure of the Eurasian continental margin.

2. Geological Background

The Taiwan orogen is evolving as a result of the latest Miocene to present collision between the Luzon Arc, located on the Philippine Sea Plate, and the Eurasian continental margin (Figure 1; Ho, 1986; Suppe, 1981). The Philippine Sea plate is colliding with the Eurasian continental margin with a c. NW46° trend at a rate of about 8.2 cm/year (Yu et al., 1997). The Taiwan orogen is divided into five roughly N-S oriented tectonostratigraphic zones that are separated by major faults (see inset; Figure 1). From west to east these zones are the following: the Coastal Plain, Western Foothills, the Hsuehshan Range, the Central Range, and the Coastal Range. In much of south-central Taiwan, the boundary between the Coastal Plain and the Western Foothills is interpreted to coincide with the mostly buried tip line of the Changhua Thrust (ChT in Figure 1). East of the Changhua Thrust, the low relief areas covered by Holocene sediments in the south and in the Pingtung Plain form thrust-top basins (C. Chiang et al., 2004) on the fold-and-thrust belt. In the study area, the Western Foothills is juxtaposed against the Central Range along the Chaochou Fault. The study area comprises the southwestern part of the Taiwan fold-and-thrust belt and foreland basin to the mountain belt (Figure 1).

The part of the Eurasian continental margin that is involved in the collision has evolved since the Eocene through several extensional episodes that predate the arc-continent collision (C. Y. Huang et al., 2012; A. T. Lin et al., 2003). With the onset of rifting in the Eocene, a number of roughly northeast southwest oriented basins (e.g., Nanjihtao and Taihsi basins) developed on the margins shelf (A. T. Lin & Watts, 2002; A. T. Lin et al., 2003; Teng & Lin, 2004) and locally accumulated up to approximately 5 km of sediments (e.g., A. T. Lin et al., 2003; Figure 1). During the Late Oligocene to Late Miocene, several extensional events further affected the outer shelf and necking zone areas of the margin (A. T. Lin et al., 2003). This resulted in an array of roughly east-northeast striking extensional faults and development of the Tainan Basin (Ding et al., 2008; Lee et al., 1993; A. T. Lin et al., 2003; Y.-J. Lin et al., 2005; Shi et al., 2008; Q. Tang & Zheng, 2010; Yang et al., 1991, 2016; Figure 1). A number of extensional faults that developed along the outer part of the margin and its slope can be traced on land (e.g., the Yichu [YF] and B [BF] faults in Figure 1), into the Coastal plain area of southwestern Taiwan (A. T. Lin et al., 2008; Yang et al., 2006, 2016), where they have been shown to affect the structure of the foreland thrust-and-fold belt (Alvarez-Marron et al., 2014; Brown et al., 2017; Camanni et al., 2016; Rodriguez-Roa & Wiltschko, 2010; Suppe, 1986; Yang et al., 2007, 2016).

3. Stratigraphy

To maintain consistency with our previous publications, we use the same chronostratigraphic nomenclature as in Brown et al. (2012, 2017) and Alvarez-Marron et al. (2014; Figure 2). For the Miocene through Holocene

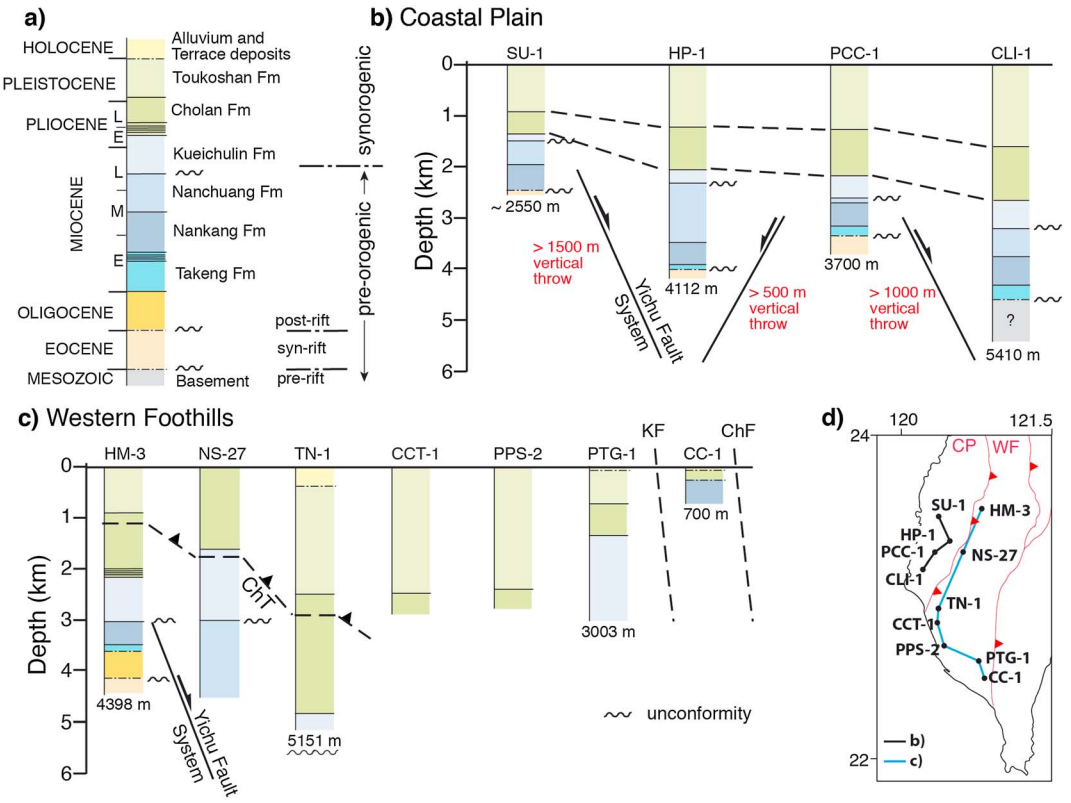

Figure 3. (a) General stratigraphy and tectonostratigraphic units showing the names of formations used in this study. (b) Stratigraphic correlation of boreholes SU-1, HP-1, PCC-1, and CLI-1 along the Coastal Plain (taken from Tensi et al., 2006; Shaw, 1996; C.-H. Tang, 1977). The interpreted approximate vertical throw accumulated by structures between boreholes is shown. (c) Stratigraphic correlation of boreholes HM-3, NS-27, TN-1, CCT-1, PPS-2, PTG-1, and CC-1 from the frontal and southern parts of the fold-and-thrust belt (taken from S. C. Chiang, 1971; Chou, 1972; Huang, 1984; S. T. Huang et al., 2004; C.-H. Tang, 1977). The location of the basal thrust in HM-3, NS-27, and TN-1 is marked as ChT (Changua thrust). (d) Inset indicates location of the boreholes. Boreholes are also shown in map of Figure 4. CP = Coastal Plain; WF = Western Foothills.

rocks, this scheme follows the stratigraphic correlation of Shea et al. (2003; Figure 2). We have subdivided a thick, latest Miocene through to Late Pleistocene-age, unit of mudstone with ribbons of sandstone that crops out in the southwestern part of the study area (the Gutingkeng Fm: Figure 2) using the chronological divisions for it that are provided by Horng and Shea (1994) and Horng (2014). The stratigraphic thickness for each formation is, where possible, taken from published borehole data (Figure 3; Chang, 1963; S. C. Chiang, 1971; Chou, 1971; S. T. Huang et al., 2004; Shaw, 1996; C.-H. Tang, 1977; Tensi et al., 2006; Yuan & Huang, 1985) and isopach maps (Chou, 1980; A. T. Lin et al., 2003; Shaw, 1996; C.-H. Tang, 1977) within the study area, and from the geological map (Figure 4).

Throughout this paper we define the basement as all pre-Eocene rifting rocks upon which the Cenozoic Eurasian continental margin was built. Basement rocks do not crop out in the study area. Although, weakly metamorphosed siliciclastic rocks and marble that have been interpreted to be Mesozoic in age have been intersected in one borehole (CLI-1) on land (Figure 3) and several boreholes offshore southwestern Taiwan (Chiu, 1975; Ho, 1988; Jahn et al., 1992; Shaw, 1996). Mesozoic rocks do, however, crop out extensively in the Central Range where they comprise predominantly marbles and schists (Ernst, 1983; Ho, 1988; Lan et al., 2008; Stanley et al., 1981). We therefore interpret these types of lithologies, capped locally by weakly metamorphosed clastic rocks, to comprise the basement beneath the study area. Within the study area, this basement can be unconformably overlain by Eocene through to Early Miocene rocks, since boreholes indicate that neither the Eocene nor the Oligocene rocks are present everywhere (Chiu, 1975; Ho, 1988; Shaw, 1996; Figure 3).

The Eocene through Early Miocene rocks do not crop out in the study area. They have, however, been intersected in several boreholes (Figure 3). In these boreholes, the Eocene and Oligocene each comprise

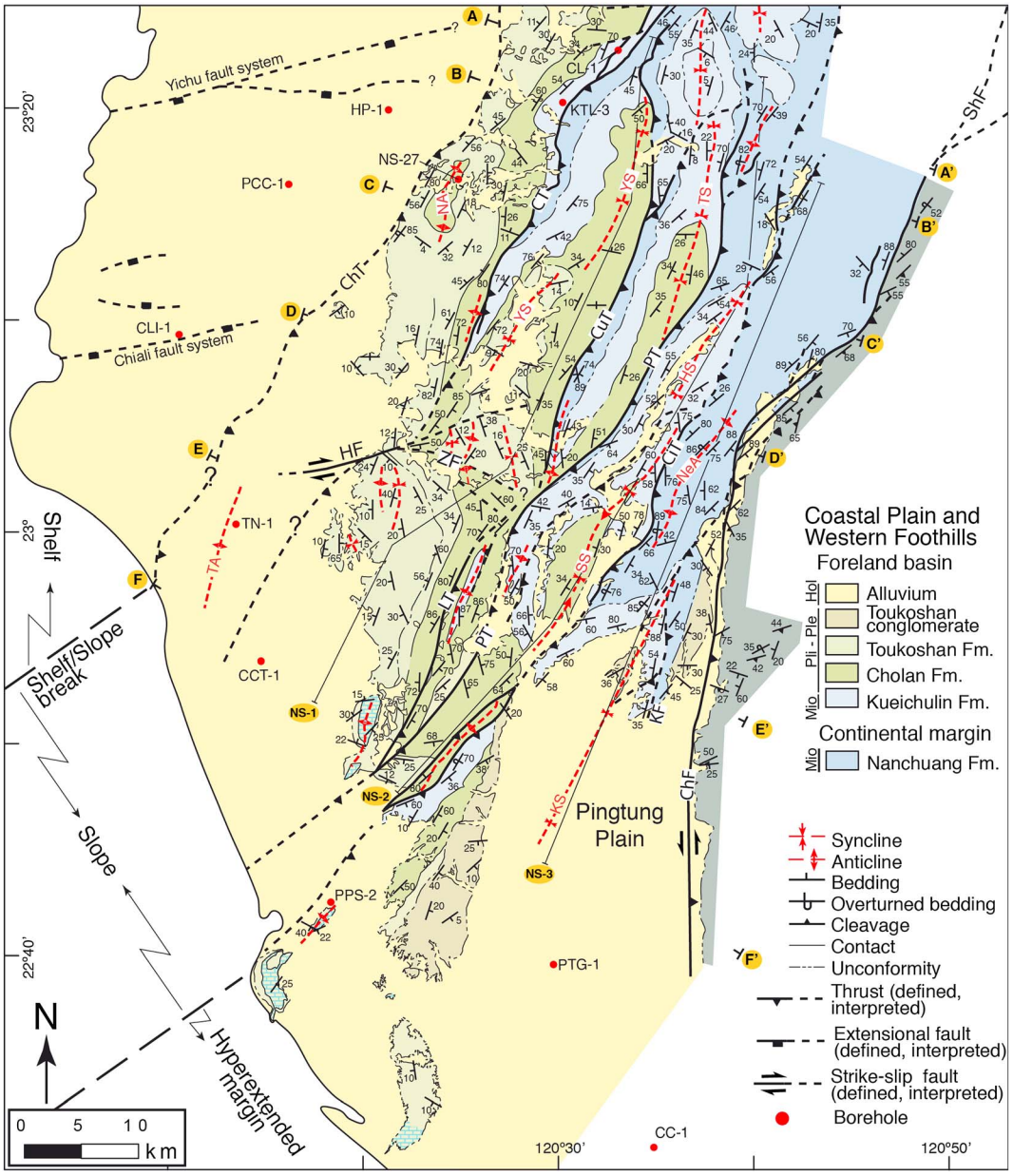

Figure 4. Geological map of southwest Taiwan. It includes the location of the geological cross sections A to F shown in Figure 6, the longitudinal cross-sections NS-1 to NS-3 shown in Figure 8, and the boreholes shown in Figure 2. Structures discussed in the text are labeled. Thrusts: ChT = Changhua thrust; CiT = Chishan thrust; CT = Chelungpu thrust; CuT = Chutochi thrust; LT = Lungchuan thrust; PT = Pingshi thrust. Faults: ChF = Chauchou fault; HF = Hsinshua fault; ZF = Zuojhen fault. Folds: NA = Niushan anticline; NeA = Neiyingshan anticlinorium; SS = Shihchangli syncline; TA = Tainan anticline; TS = Tingpinglin syncline; YS = Yuching syncline; HS = Hsiaolin syncline; KS = Kuanglin synform.

up to several hundred meters of predominantly sandstone and shale, although they may be thicker in certain areas. The Early Miocene Takeng and Nankang formations comprise several hundred meters to nearly 1,000 m of sandstone and shale (Shaw, 1996; Yang et al., 2014; Figure 3).

The outcropping stratigraphy of the study area (Figure 4) comprises Middle Miocene through Holocene clastic rocks with, in the extreme southwest, small, isolated, and laterally discontinuous outcrops of limestone. In the north and east, the Middle to Late Miocene Nanchuang and the Late Miocene to Early Pliocene Kueichulin formations dominate (Figure 4). The Nanchuang Formation is made up of thin- to thick-bedded sandstone intercalated with shale. Its thickness varies widely across the study area, ranging

from several hundred meters to more than 2,000 m. These changes in thickness have been interpreted to be related to deposition of the Nanchuang Fm in marine extensional basins during the Middle Miocene development of the Tainan Basin (A. T. Lin et al., 2003; Yang et al., 2006). The Nanchuang Fm is unconformably overlain by the Kueichulin Fm (A. T. Lin et al., 2003).

The Kueichilin Fm comprises shallow marine facies, thin to very thick-bedded muddy sandstone and sandy mudstone. In agreement with A. T. Lin et al. (2003), we take the Kueichulin Fm to mark the onset of synorogenic sedimentation in the foreland basin because of the regionally developed unconformity at its base that has been interpreted to be related to plate flexure caused by orogenic loading (A. T. Lin & Watts, 2002; Tensi et al., 2006). This is in contrast to Teng (1987), Covey (1986), and Hong (1997), who suggest that the onset of foreland basin sedimentation occurred during the Early Pliocene, and is recorded by the appearance of slate clasts in the Chinshui shale at the base of the Cholan Fm. The Kueichilin Fm crops out extensively in the north and central part of the study area (Figure 4). It thickens significantly from east to west and from north to south, with thickness ranging from ~150 m to more than 3,000 m (Figures 3 and 4; S. C. Chiang, 1971). The Kueichilin Fm is conformably overlain by the Early Pliocene to Early Pleistocene marine facies Cholan Fm. The Cholan Fm may reach more than 4,000 m in thickness and is made up of interbedded mudstone, shale, and muddy sandstone. The Cholan Fm is overlain by the Early Pleistocene marine facies Toukoshan Fm, a coarsening upward sequence made up of thick-bedded muddy sandstone and shale that, upward, becomes interfingered with, and locally unconformably overlain by conglomerate. The Toukoshan Fm contains a number of regional-scale internal unconformities and can reach more than 3,000 m in thickness (Figure 4). The Toukoshan Fm is overlain by Holocene-age fluvial gravels that, in places, are several hundred meters thick.

4. Methodology

The structural analyses and interpretations that follow are based on our new geological mapping (Figure 4). This mapping is the southern continuation of previous work by our group in south-central Taiwan (Alvarez-Marron et al., 2014; Brown et al., 2012). Field mapping was carried out at 1:50,000 scale using the geological maps of the Central Geological Survey of Taiwan as a base. The final map was drawn at 1:50,000 scale using the chronostratigraphic scheme shown in Figure 2. For clarity, in Figure 4 only representative structural data are shown; a 1:100,000 scale map with all of our bedding dip data can be found in supporting information Figure S1 and the bedding database in Table S2. Major thrusts and their names have been correlated from north to south (see Ho, 1986, for a similar correlation). In the description of the structure that follows, the study area has been divided into a number of structural units (Figure 5).

Six balanced and restored cross sections, oriented perpendicular to the regional strike of structures (bedding, thrusts, and major fold traces), have been constructed using the geological map, field structural data, and the standard section construction techniques (Dahlstrom, 1969; De Paor, 1988; Hossack, 1979; Figures 6 and 7). Where possible, additional constraints were placed on the structure and the stratigraphic thicknesses from published borehole data (Figure 3). Boreholes were projected along the bedding strike onto the cross sections (Figure 6). In an iterative process, together with the construction of cross sections, three roughly north-south, strike-parallel sections (NS-1, NS-2, and NS-3 in Figure 4) were also constructed (Figure 8), and maps of the basal thrust, branch line maps, and stratigraphic cutoff maps were drawn (Figures 9a and 9b). This iterative approach insured a 3-D consistency of the structural interpretation and assured the viability of the cross sections. The cross sections have been line balanced (while conserving area) and restored (Figures 6 and 7), with the exception of section A-A′, which was not restored because it crosses the oblique Yichu ramp (see below; Figure 9a). In all the restored sections the western pin line was placed in the undeformed rocks to the west of the Changhua thrust tip line. The sections have been restored to a horizontal top of the Kueichulin Fm, a regional-scale marker that can be mapped throughout much of the study area (Figure 4). Minimum shortening estimations in the cross sections, which is a by-product of their balancing and restoration, is briefly presented but is not the focus of this study.

Finally, to place some constraint on the depth to, and the geometry of, the top of the basement, we interpret it to approximately coincide with a *P* wave (*Vp*) velocity of 5.2 km/s (Figures 6 and 8), which is taken from the 3-D tomography model of Kuo-Chen et al. (2012). See Brown et al. (2017) for a more extensive argumentation for using this velocity as a proxy for the top of the basement. We stress, though, that this isovelocity surface is only meant to help with the interpretation of the location of the top of the basement rocks at depth and that

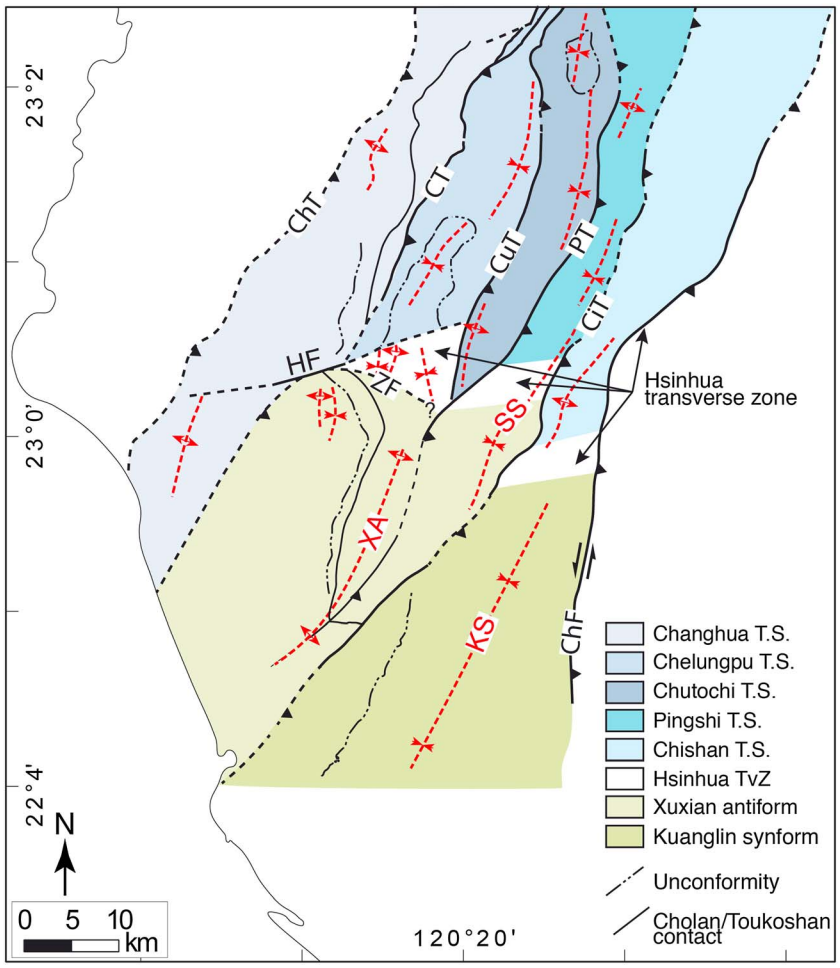

Figure 5. Structural units of the southern Taiwan fold-and-thrust belt described in the text. The Hsinhua transverse zone marks the transition from a mostly emergent thrust system in the north to a southern area dominated by the Xuxian antiform and the Kuanglin synform where large areas of the thrust sheets are buried.

it may not coincide with the depth to basement determined using the section construction methods (see the dashed red lines in Figures 6 and 8).

Before continuing with the presentation and discussion of the structure of the fold-and-thrust belt in the following sections, we feel that some remarks about the uncertainties involved in the interpretations are appropriate. The primary data set for all the interpretations that follow is the geological map (Figure 4). During our mapping we have made a number of assumptions that could have led to errors in the map. These include (1) making a chronostratigraphic correlation that link different rock units and facies together on the basis of age and (2) correlating thrusts and stratigraphic contacts along strike through difficult terrain with, locally, sparse outcrop information. Any errors generated in this way were then introduced into the cross sections and these, together with the general assumptions involved in the cross-section construction, such as plane strain, no layer parallel slip, the fold mechanism, a horizontal top for the Kueichulin, or the depth to the basal thrust calculations, also lead to errors in the cross sections. A weakly constrained stratigraphic template precluded doing rigorous area balancing. See also Judge and Allmendinger (2011) and Groshong et al. (2012) for a general discussion of cross-section balancing and its uncertainties. Furthermore, we did not have access to either the original borehole descriptions or their locations. The borehole information presented here has been taken from various publications and may therefore contain significant errors. A further, and important uncertainty is the use of a *Vp* of 5.2 km/s as a proxy for the top of the basement. The uncertainties inherent in the velocity model, its low resolution (20 km by 20 km by 10 thick) compared to that of the surface geology, and the petrophysical assumptions made for conversion of *Vp* to rock type (e.g., Brown et al., 2017) all mean that

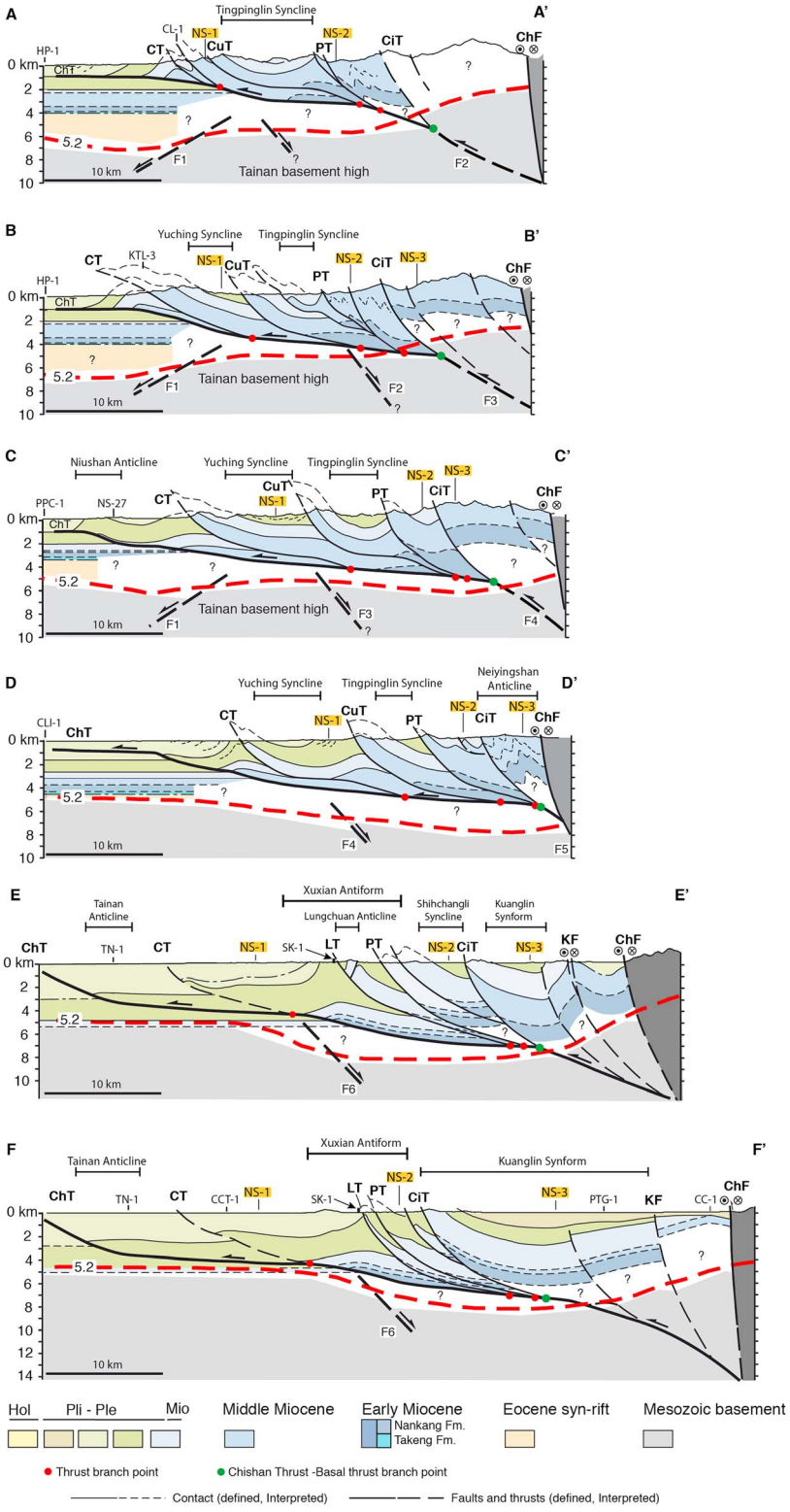

Figure 6. Geological cross sections through the southwestern Taiwan fold-and-thrust belt. Their locations are shown in Figure 4. They include the projected location of the boreholes used for their construction and the branch points (red dots) of individual thrusts. The branch point of the CiT (green dots) is interpreted to mark the ramp down into the basement of the basal thrust. Branch points were used to construct the branch line map in Figure 9. Red dashed line is the 5.2 km/s *Vp* contour from the TAIGER local tomography. Faults interpreted in the basement are labeled F1 to F6 for correlation in Figures 7 and 8. Abbreviations are as in Figure 4.

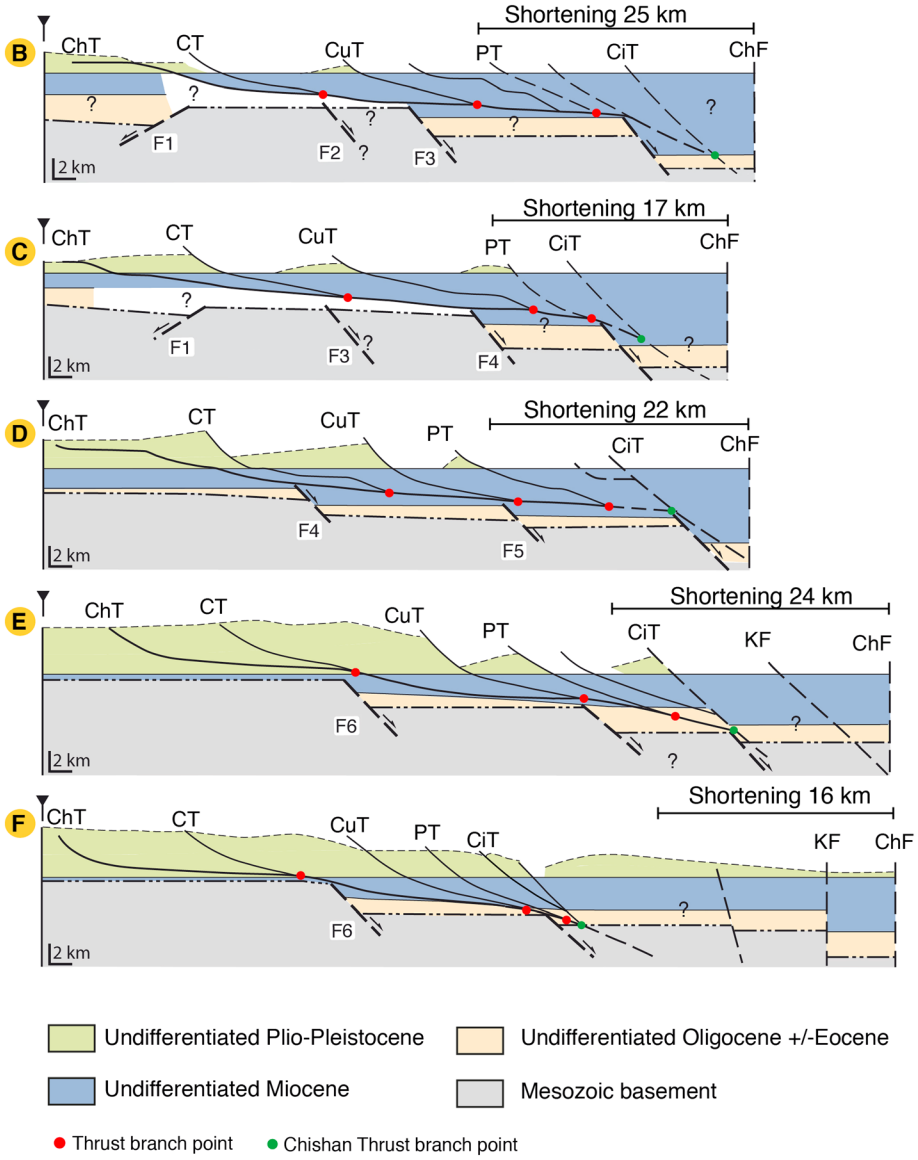

Figure 7. Restored sections B to F. The sections have been restored using bed-length balancing of top and base of Kueichulin Fm and are area balanced for the rest of the Miocene units above the basal thrust. Faults interpreted in the basement are labeled F1 to F6 and correspond to those in Figures 6 and 8. Abbreviations are as in Figure 4.

this assumption for the basement-cover interface may not be valid everywhere. While we have taken care to keep all of these uncertainties to a minimum, we nevertheless present both the map and the cross sections as interpretations, the restorations as approximations, and the displacement and shortening calculations as minimums.

5. Structure of Southwestern Taiwan

5.1. Surface Geology

The study area covers the Coastal Plain and the Western Foothills (including the area covered by Holocene sediments in the south and on the Pingtung Plain) of southwestern Taiwan (Figures 1 and 4). In this area, the fold-and-thust belt is bounded to the east by the Chaochou fault and in the west by the buried tip line of the Changhua thrust (CT; Figure 4; see also, Ching et al., 2011; Rodriguez-Roa & Wiltschko, 2010; Shyu et al., 2005; Yang et al., 2007; Yu et al., 1997). Seismicity to the west of the Changhua thrust indicates, however, that deformation is also taking place beneath this westernmost part of the Coastal Plain (e.g., Brown et al., 2017;

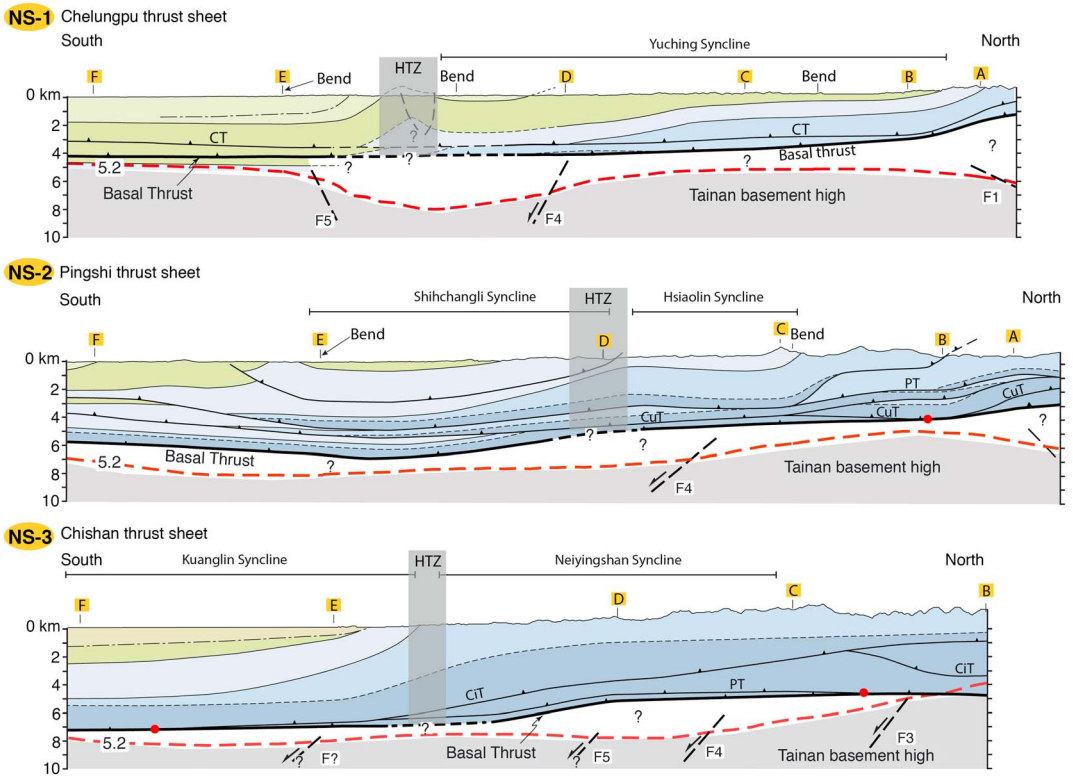

Figure 8. North-south geological cross sections. NS-1 along the Chelungpu thrust sheet, NS-2 along the Pingshi thrust sheet, and NS-3 along the Chishan thrust sheet. The area corresponding to the Hsinhua transverse zone (HTZ) of Figure 5 is shown by the gray shaded box. The dashed part of the basal thrust below the HTZ that is marked by a question mark indicates uncertainty about what the interaction between the two is. Faults labeled F1 to F6 correspond to those in Figures 6 and 7. Legend is as in Figure 6. Red dashed line is the 5.2 km/s *Vp* contour from the TAIGER local tomography. Abbreviations are as in Figure 4.

Camanni et al., 2016; Shyu et al., 2005). In terms of the morphological parts of the continental margin that are entering into the deformation, the study area (Figures 1 and 4) comprises the outer part of the shelf, as well as the on land projections of the shelf-slope break, and part of the slope area. In structural terms it comprises part of the necking zone and the beginning of the hyperextended part of the margin (e.g., Brown et al., 2017; Lester et al., 2014; McIntosh et al., 2014). The boundaries between all of the morphological parts of the margin, as well as the extensional fault system on the necking zone, are oriented at a high angle to the structural grain of the developing fold-and-thrust belt (Figures 1 and 4; Lee et al., 1993; A.T. Lin et al., 2003; Yang et al., 1991, 2016). On the basis of borehole and reflection seismic data, a number of the roughly east-northeast striking extensional faults mapped in the offshore have been traced on land, into the Coastal Plain (the B, Yichu, and Chiali fault systems; e.g., A. T. Lin et al., 2003; Yang et al., 2014, 2016; Figures 1 and 4).

The structural grain of the fold-and-thrust belt in southwestern Taiwan is roughly north-northeast striking, with several pronounced, sigmoidal, en echelon changes toward a more northeast strike (Brown et al., 2017; Figure 4). It has a buried thrust front and all major thrusts are interpreted to extend southwestward into the offshore where they form a marine accretionary complex (C. Chiang et al., 2004; A. T. Lin et al., 2008; Shyu et al., 2005). The surface structure of the study area is that of an imbricate thrust system, but with a pronounced north-south change in structural architecture that is presented and discussed in detail below. In the north, the study area comprises five thrust sheets: the Changhua, Chelungpu, Chutochi, Pingshi, and Chishan thrust sheets, whereas in the south it consists of the Changhua thrust sheet, the Xuxian antiform, and the Kuanglin synform (Figure 5). Below, we will present evidence of, and arguments for, the north-south change in structural architecture taking place across a roughly east-west striking zone that we call the Hsinhua transverse zone (Figure 5). In the southern part of the study area, large areas of the thrust sheets

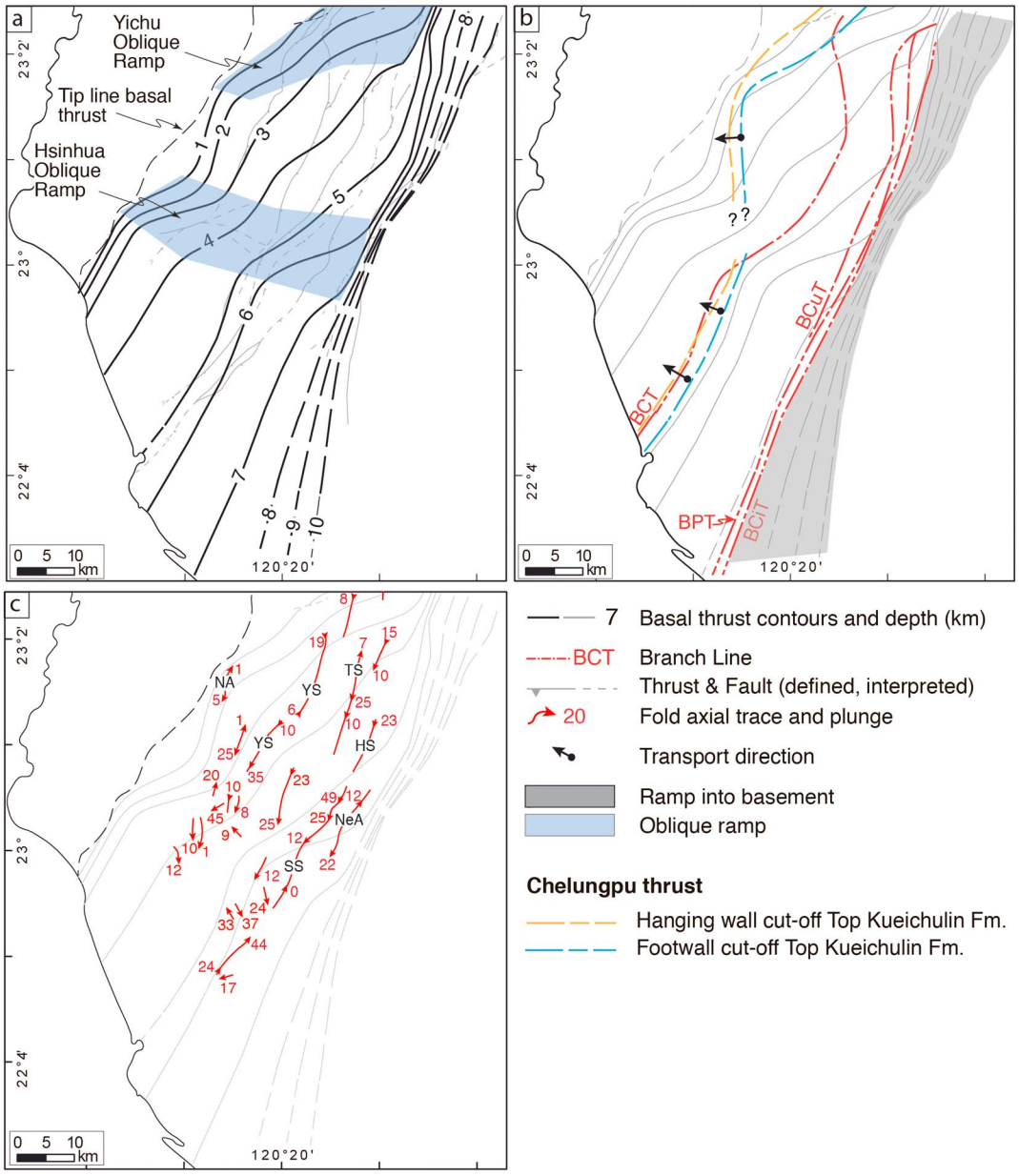

Figure 9. (a) Structural contour line (in km) map of the basal thrust. Thrusts and faults are shown in light gray. (b) Hanging wall and footwall cutoff lines of the top of Kueichulin Fm in the norhtern and southern areas, and branch lines (red) of the Chelungpu, Pingshi, Chutochi, and Chishan thrusts are shown superposed on the basal thrust contour lines. The arrows show the assumed displacement direction, which is interpreted to be perpendicular to the frontal stratigraphic cutoffs. The area where the basal thrust is interpreted to ramp down into the basement is labeled in gray. This ramp starts from the BCiT that is at about 5 km in the north and deepens southward till more than 7 km. (c) Fold axial traces and plunge of the main folds superimposed on the basal thrust contour map. Abbreviations are as in Figure 4.

(all of the proposed continuation of the Changhua thrust sheet, as well as the Kuanglin synform) are buried by Holocene sediments. Below we give a description of the surface geology of each of these, followed by an interpretation of the subsurface structure in section 5.2.

The Changhua thrust sheet (Figure 5) is bounded in the west by the buried Changhua thrust and in the east by the Chelungpu thrust (ChT and CT, respectively, in Figures 4 and 5). It crops out only in the northern half of the study area where it is composed of predominately Cholan and Toukoshan formations, with a minor amount of Kueichulin Fm in the northeast (Figure 4). The southern half is covered by Holocene sediments,

and the trace of the buried Changhua thrust in Figure 4 is interpreted from small topographic highs and published reflection seismic data (see also, S. T. Huang et al., 2004; Shyu et al., 2005). In the north, from east to west, the structure of the Changhua thrust sheet is that of a steep to gently west dipping monocline that is interrupted only by the doubly plunging Niushan anticline (NA in Figure 4), whose western limb is locally steep to overturned. In the southeastern part of the outcropping Toukoshan Fm there is a regional-scale unconformity of Late Pleistocene age that juxtaposes shallow marine sandstone and shale against fluvial sandstone and conglomerate. There are a number of smaller, local, unconformities developed throughout the Pliocene and Pleistocene sequences in the Changhua thrust sheet (W.-S. Chen et al., 2001). In the area covered by Holocene sediments, the roughly east-northeast striking Hsinhua fault (Figure 4) represents the dextral oblique-slip surface rupture of the 1946 Hsinhua earthquake (Bonilla, 1975; Shyu et al., 2016). In the very southwest, the Tainan anticline does not crop out but is marked at the surface by a small area of low topography. It has been imaged in reflection seismic data (S. T. Huang et al., 2004). We interpret the Tainan anticline to be forming in the immediate hanging wall of the Changhua thrust (see also M.-H. Huang et al., 2009; Lacombe et al., 1999).

The Chelungpu thrust sheet (Figure 5) is bounded by the Chelungpu thrust (CT) in the west and by the Chutochi thrust (CuT) in the east (Figure 4). It contains Middle Miocene through Pleistocene rocks that are overlain by Holocene sediments. The Chelungpu thrust sheet is comprised predominately of the gently to moderately south-southwest plunging Yuching syncline (YS in Figure 4). In the immediate hanging wall of the Chelungpu thrust, along the western limb of the Yuching syncline, the Nanchuang and Kueichulin Fms dip steeply to the southeast before the dips shallow in the Cholan Fm where there are numerous local southeast dipping unconformities. Along the eastern limb of the Yuching syncline, bedding dips change direction and amount from north to south, and unconformities are not common. In the core of the Yuching syncline, moderately to steeply dipping Cholan Fm rocks are overlain by gently south dipping Toukoshan Fm along an Early Pleistocene-age unconformity (Figure 4). Southward, the Chelungpu thrust sheet, ends against the Hsinhua fault (HF in Figure 4).

The Chutochi thrust sheet (Figure 5) is bounded in the west by the Chutochi thrust (CuT) and in the east by the Pingshi thrust (PT; Figure 4). The Chutochi thrust sheet is composed of Middle Miocene through Early Pleistocene rocks. The structure of the Chutochi thrust sheet is dominated by the Tingpinglin syncline (TS in Figure 4), a gently south plunging syncline cored in the south by Cholan Fm. In the northernmost part of the thrust sheet, the Tingpinglin syncline is weakly developed within the Kueichulin Fm, which also contains a marked internal unconformity. Unconformities are not found in the Cholan Fm. The northern part of the Chutochi thrust sheet is cut by a connecting splay between the Chutochi and Pingshi thrusts. Southward, the Chutochi thrust ends against the Pingshi thrust, which cuts across both limbs of the Tingpinglin syncline.

The Pingshi thrust sheet (Figure 5) is bounded in the west by the Pingshi thrust (PT) and in the east by the Chishan thrust (CiT; Figure 4). In the north, its internal structure and the traces of both the Pingshi and Chishan thrusts are not well resolved because of difficult access. Despite this, a number of small splays and their related folds have been identified along the margins of the thrust sheet in this area. The structure of the Pingshi thrust sheet is dominated by the moderately southwest plunging Hsiaolin syncline and the doubly plunging Shihchangli syncline (HS and SS, respectively in Figure 4). On the basis of an increased thickness of the Kueichulin Fm along the western limb of the Hsiaolin syncline, we interpret the presence of a minor thrust that thickens the Kueichulin Fm and causes minor folding in its hanging wall. We interpret the Pingshi thrust to continue southward into the eastern limb of the Xuxian antiform (PT in Figure 4).

The Chishan thrust sheet (Figure 5) is bounded by the Chishan thrust (CiT) in the west and by the Chaochou Fault (ChF) in the east (Figure 4). Because of difficult access, only the margins of the northernmost part of the Chishan thrust sheet have been looked at in this study. In this area, the Nanchuang Fm rocks are intensely folded and faulted. The southern part of the Chishan thrust sheet comprises tightly folded and faulted rocks of the Nanchuang Fm, forming the west verging, south-southwest plunging Neiyingshan anticlinorium (NeA in Figure 4). We interpret the Chishan thrust sheet to continue southward beneath the Pingtung Plain, although with a prominent along-strike change from the Neiyingshan anticlinorium to the Kuanglin synform (Figure 4).

Southward, increasing amounts of the fold-and-thrust belt become buried beneath the Holocene synorogenic sediments (Figure 4). This means that we have less outcrop control on the structure. But with the help of published borehole data (S. C. Chiang, 1971; C. Chiang et al., 2004; Chou, 1972; S. T. Huang et al., 2004; C.-H.

Tang, 1977) and reflection seismic profiles (S. T. Huang et al., 2004) we have interpreted a generalized structure in the areas without outcrop, such as the Changhua thrust sheet and the Kuanglin synform. These interpretations are, however, highly speculative. Nevertheless, it is apparent that the Chelungpu thrust sheet ends southward against the Hsinhua fault. South of the Hsinhua and Zoujhen (ZF) faults, bedding dips are steep to gentle toward the west to southwest before taking on a southward dip as the contact between the Cholan and Toukoshan Fms turns to strike east-west, forming a south plunging fold closure (Figure 4). We name this fold the Xuxian antiform. The core and the eastern limb of the Xuxian antiform is cut by the Lungchuan, Pingshi, and Chishan thrusts (LT, PT, and CiT, respectively, in Figure 4). Since it does not appear to continue northward or to merge with the Chutochi thrust, we interpret the Lungchan thrust sheet to form a horse in the footwall of the Pingshi thrust. The Xuxian antiform is composed of Late Miocene through Pleistocene rocks and is bounded to the west by the buried Chelungpu thrust and to the east by the Chishan thrust. Along the western limb of the antiform, there is a pronounced west to southwest dipping Late Pleistocene-age unconformity within the Toukoshan Fm that marks a change from shallow marine to predominately fluvial facies sediments. Smaller, local unconformities are widespread within the shallow marine facies rocks of the lower Toukoshan and Cholan formations.

The Kuanglin synform is bounded by the Chishan thrust in the west and the Chaochou fault in the east (Figure 4). It crops out only along its western side and its hinge area in the north. In the west, the Chishan thrust juxtaposes moderately to steeply southeast dipping Late Miocene through Pleistocene rocks against the eastern flank of the Xuxian antiform. Along the western limb of the synform, there is a marked Late Pleistocene erosional unconformity along which fluvial facies Toukoshan Fm conglomerate overlies shallow marine sandstone of the same formation. In the north, the hinge zone of the Kuanglin synform is composed of steeply southeast dipping and west dipping Kueichuin Fm thick-bedded sandstone, with and isolated outcrop of Late Pleistocene-age, slate-bearing conglomerate.

From the surface geology, it is clear that there is an important change in structural architecture from the thrust sheets in the north to the Xuxian antiform in the south, and from the Neiyingshan antiform in the north to the Kuanglin synform in the south. The zone across which this change takes place is not a single, discrete structure, but is composed of a suite of structures whose northern and southern boundaries are sometimes transitional into the regional-scale structures on either side. In the west, it comprises the roughly east-northeast striking, dextral strike-slip Hsinhua fault (HF in Figures 4 and 5), which extends at least from the surface rupture of the 1946 Hsinhua earthquake (solid line in Figure 4) eastward to the Chutochi thrust. The Zuojhen fault (ZF in Figures 4 and 5) is a zone that consists of several roughly east-southeast striking faults that join the Hsinhua fault in the west to form a conjugate strike-slip fault system. The Zuojhen fault can be traced eastward to the Pingshi thrust. In between the Hsinhua and Zuojhen faults, the structure comprises a series of north-northwest trending, upright folds. Eastward, the Pingshi and the Chishan thrusts display marked sigmoidal bending of their surface traces and of the bedding in their hanging walls. The Pingshi thrust cuts across both limbs of the Tingpinglin syncline, and the Chutochi thrust is cut by it. Between the area of sigmoidal bending of the Pingshi and Chishan thrusts, the Shihchangli syncline (SS in Figure 4) plunges moderately southward (approximately 50°) and gently northward (<5°) in its northern and southern parts, respectively (Figure 4). Eastward, in the hanging wall of the Chishan thrust, where it goes through a change in strike, the Neiyingshan antiform terminates abruptly southward and the Kuanglin synform replaces it (NeA and KS, respectively, in Figure 4). We call this zone of structural changes the Hsinhua transverse zone (Figure 5). We use the term transverse zone, as defined by Thomas (1990), to be *a systematic alignment of lateral connectors between two sets of differing structures*. According to this definition, a transverse zone can be manifested as a suite of possible structures (these are described for the Hsinhua zone below) with a range of probable causes (which we will discuss later, in section 6).

5.2. Subsurface Structure

Because of the north-south differences in structure across the study area, we divide the description that follows into that to the north of the Hsinhua transverse and that to the south. Nevertheless, throughout the study area, we interpret the tip line of the Changhua thrust (ChT) to also be that of the basal thrust (Figure 6). North of the Hsinhua transverse zone, the basal thrust in the west forms a shallow (~1-km depth) flat within the Pliocene or Pleistocene rocks before it ramps down eastward into the Middle Miocene (sections A through D in Figure 6). In this part of the study area, we interpret the juxtaposition of the

Chelungpu, Chutochi, and Pingshi thrust sheets, with their leading thrusts located predominately in the Nanchuang Fm, together with the similar (although slightly increasing toward the east) erosion level in the cores of their respective synclines, to indicate that the basal thrust dips about 4° toward the east within the Middle Miocene rocks beneath these thrust sheets. Eastward, on the basis of the increased thickness of strongly folded Miocene rocks in its hanging wall, and on the uplift of higher velocity rocks (>5.2 km/s), we interpret a ramp into the basement to occur along the Chishan thrust (Figure 6). Displacement (measured as the distance that the top of Kueichulin moved along a thrust surface) along individual thrusts in section A through D generally decreases southward and increases eastward. Note, however, that we have poor control on section A and limited information for the Chishan thrust where this cutoff is not found (Figure 6). From the balanced and restored cross sections, we estimate the minimum shortening in this part of the fold-and-thrust belt to be between 17 and 25 km (Figure 7).

South of the Hsinhua transverse zone, especially along much of section F and the western part of section E, the fold-and-thrust belt is poorly exposed, being buried by Holocene sediments in thrust-top basins. We therefore have variable control on the surface structure south of section E with which to place constraints on the subsurface geometry of the thrust system. Nevertheless, borehole TN-1 (Figure 3) shows that the Cholan and Toukoshan formations thicken significantly compared to north of the Hsinhua transverse zone, whereas along the western limb of the Xuxian anticline the Miocene thins or even disappears. In agreement with the interpretation of M.-H. Huang et al. (2009) and Mouthereau et al. (2001), we interpret the basal (Changhua) thrust to be listric along its westernmost part before forming a flat within the Cholan Fm at ~4-km depth (Figures 6e and 6f). Eastward, we interpret it to ramp down into the Middle Miocene rocks beneath the Xuxian antiform, since these rocks are exposed in its core and in thrust sheets along its eastern flank. Based on the shallowing of the 5.2 km/s isovelocity line, we interpret the basal thrust to ramp down into the basement east of the Chishan thrust (Figure 6).

The Kuanglin synform is only exposed along part of its western flank and in the core of the synform in the north (Figure 4). On the basis of our surface structural data, boreholes PTG-1 and CC-1 (Figure 4), and following Mouthereau et al. (2001) and Chiang et al. (2004), we interpret the Kuanglin synform to widen southward into a broad, open syncline with only minor internal deformation. Despite limited control on stratigraphic cutoffs we nevertheless interpret displacement to increase eastward in Section E and calculate a minimum shortening of around 24 km. Estimates of displacement and shortening for Section F are highly speculative.

In the strike-parallel sections (Figure 8), we interpret the transition in structure across the Hsinhua transverse zone, with the exception of NS-1, to be smooth, continuous, and marked by a general southward dip of all contacts. Although, the details of this area of transition may be more complex, and it cannot be fully resolved with the current data set. Because of this uncertainty, in Figure 8 we show the Hsinhua transverse zone as a gray area and the basal thrust as a dashed line. In Section NS-1, the area of the Hsinhua-Zoujhen fault system displays a pronounced, asymmetrical, and faulted anticline that we interpret to be forming in a dextral, positive flower structure that possibly cuts the basal thrust. In Sections NS-2 and NS-3, however, it is not clear how the transverse zone is reflected in the subsurface structure. Nevertheless, on the basis of the balanced cross sections (Figure 6), we interpret the basal thrust to deepen by up to 2 km from north to south, across the Hsinhua transverse zone (Figure 8), and the borehole data (Figure 2) show a thinning of the Middle Miocene rocks, in particular the Nanchuang Fm, and the concomitant thickening of the Kueichulin, Cholan, and Toukoshan formations.

By contouring the basal thrust from the cross- and strike-parallel sections, we see that it dips gently toward the southeast, with two pronounced sigmoidal changes in strike of the depth contours that form what we call the Yichu and Hsinhua oblique ramps (Figure 9a). From north to south, the branch line of the Chelungpu thrust undergoes a marked change in strike, from nearly downdip along the Yichu ramp to roughly parallel to the basal thrust contours across the Hsinhua ramp (Figure 9b). The branch lines of the Chutochi and Pingshi thrusts are oblique to the basal thrust contours across both the Hsinhua and Yichu ramps. Both ramps end at the Chishan thrust as, on the basis of the shallowing of the 5.2 km/s isovelocity surface, this thrust is interpreted to ramp down into the basement (gray are in Figure 9b). From our data we can only determine the hanging wall and footwall cutoffs with respect to the basal thrust for the Kueichulin Fm along the Chelungpu thrust (Figure 9b). In the north, these cutoffs undergo significant changes in strike and location with respect to the Chelungpu branch line compared to farther south. In the north, the cutoffs parallel the

basal thrust contours along the Yichu ramp, reaching up to nearly 15 km west of the branch line at a depth of 1 to 2 km. They then take on a nearly north-south strike, cutting obliquely across the basal thrust contours along the Hsinhua ramp to become parallel to them along the frontal ramp where they are east of the Chelungpu branch line at a depth of 5 to 6 km. The transport direction, which is calculated to be perpendicular to the footwall and hanging wall cutoffs, is approximately westward in the north, becoming more west-northwest in the south (Figure 9b). These changes in orientation and location of the cutoffs relative to the thrust branch line provide further evidence that the Yichu and, in particular, the Hsinhua oblique ramps have an important effect on the structure of the thrust system. Although these determinations of transport direction provide important kinematic information for our structural model, the information is limited since we were not able to resolve the location of the cutoffs across the Hsinhua oblique ramp, nor the cutoffs for other thrusts. Nevertheless, the transport directions obtained in this way are in good agreement with long-term displacements fields determined by Lacombe et al. (1999, 2001) and modeled with GPS data by Ching et al. (2011). There are also significant changes in fold style, plunge direction, and plunge amount associated with both the Yichu and the Hsinhua oblique ramps (Figure 9c). For example, in the northern part of the study area, the fold structure is dominated by long, shallowly plunging synclines with mildly sinuous axial traces (YS and TS in Figure 9c) as they cross the Yichu oblique ramp, but they terminate abruptly at the Hsinhua oblique ramp. Here axial traces are short and, where there are sharp bends in the oblique ramp, folds have overall moderately to gently northwest or southeast plunges. A notable exception to this is the periclinal Shihchangli syncline (SS in Figure 9c) whose axial trace undergoes marked changes in plunge amount and direction as it crosses the Hsinhua oblique ramp, giving it a geometry common to folds draping over lateral footwall ramps (e.g., Alvarez-Marron, 1995).

The structure beneath the basal thrust is highly interpretative throughout the study area, and to show this, we have left parts of the sections blank (Figures 6 and 8). Nevertheless, we feel that it is essential for understanding the potential role played by the basement in the deformation to attempt some constraints on the structure beneath the basal thrust. From the borehole data and the surface geology (Figures 3 and 4), it is clear that there are changes in thickness of the Miocene rocks from one thrust sheet to another. These changes in thickness have been interpreted here, and in a number of other studies in southwest Taiwan (Alvarez-Marron et al., 2014; Rodriguez-Roa & Wiltschko, 2010; Suppe, 1986; Yang et al., 2007, 2016), to indicate the presence of roughly east-northeast striking, Miocene-age, extensional faults that had developed on the outer shelf, and slope areas of the continental margin (e.g., A. T. Lin et al., 2003; Yang et al., 1991). In our sections (Figures 6 and 8) we have also interpreted changes in depth of the 5.2 km/s isovelocity line to coincide with several of these extensional faults allowing us, in a number of cases, to trace them from one section to another (e.g., F1 and F3 in Figures 6–8) where they affect the geometry of the basement-cover interface proxy. We stress, however, that the details of the basement structure remain speculative.

6. Discussion

An important step for understanding the 3-D structure of a fold-and-thrust belt is to be able to link its mapped surface structure with a well-constrained interpretation of its structure at depth. In general, this is accomplished by the iterative construction of serial cross- and along-strike sections (as described in section 4). Further insights into the subsurface structure can then be obtained by making maps of stratigraphic cutoffs and thrust branch lines off the basal thrust (e.g., Boyer & Elliott, 1982; Elliott & Johnson, 1980; Hossack, 1983; Oncken et al., 1999; Srivastava & Mitra, 1994; Woodward, 1986). This workflow results in an integrated structural model of a fold-and-thrust belt that, while nonunique, reduces the uncertainties inherent in a 2-D model composed of serial cross sections alone. From such a structural model we can make reasonably well-constrained interpretations of the structure and make inferences about the geological processes that went into the development of the structural architecture of the fold-and-thrust belt in southwest Taiwan. Of these processes, the reactivation of faults derived from a continental margin has been shown to be particularly important in many fold-and-thrust belts from around the world, including Taiwan (see the references in the section 1). In the discussion that follows, we focus on the along-strike change in structure that takes place from the Chelungpu, Chutochi, Pingshi, and Chishan thrust sheets in the north to the Xuxian antiform and the Kuanglin synform in the south, arguing, as we did in section 5.1, that this change takes place along a transverse zone. We then go on to argue that this transverse zone is reflecting the response of the deformation in the fold-and-thrust belt to structural and morphological features inherited

10.1029/2017TC004910

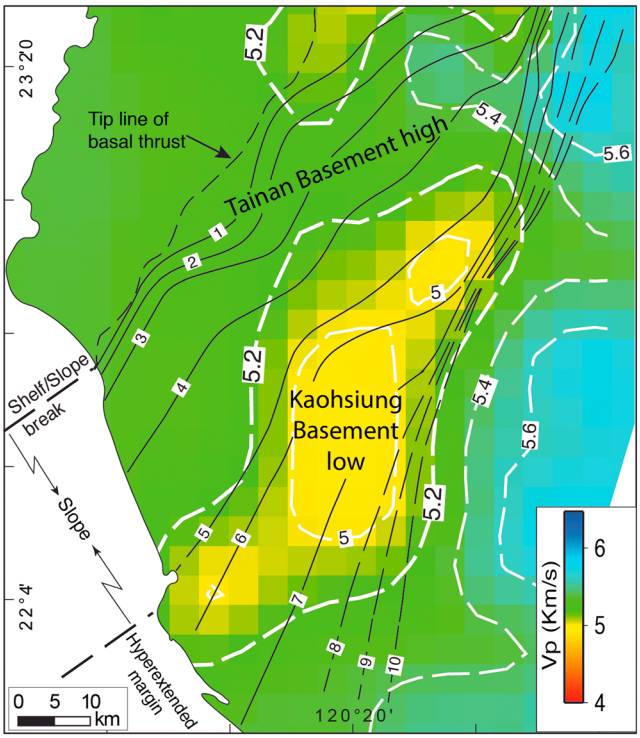

Figure 10. The 6-km depth slice of the *Vp* tomography model of Kuo-Chen et al. (2012) for the south western Taiwan area. Several isovelocity lines in km/s are shown in white dashed line, including the 5.2 km/s represented in sections shown in Figures 6 and 8. The superposed thin black lines correspond to the depth contours in km of the basal thrust.

from the deforming Eurasian continental margin. Other workers have also interpreted transfer zones in this part of the fold-and-thrust belt and interpreted them to be the result of the reactivation of preexisting faults on the margin (e.g., Deffontaines et al., 1997; Lacombe et al., 1999). While our field data do not support the model of transfer zones as proposed by Deffontaines et al. (1997), Lacombe et al. (1999, 2001), Mouthereau et al. (1999, 2002), and Mouthereau and Lacombe (2006), it is noteworthy that the dip directions of the Yichu and Hsinhua oblique ramps (Figure 9) roughly coincide with the interpreted strikes of their Chiayi and Chishan transfer zones. Furthermore, S. T. Huang et al. (2004) interpreted sigmoidal bends in the basal thrust near our Hsinhua oblique ramp to be related to basement highs, going on to suggest that these bends might be the cause of the changes in the GPS displacement field in this area.

If we accept that the suite of structures mapped at the surface (east-northeast striking faults, sigmoidal bends of thrusts, periclinal folds, etc.) and in the subsurface (an oblique ramp in the basal thrust, the change in location and depth of stratigraphic cutoffs, and so on) form a transverse zone (Hsinhua) across which the important north to south change in the structure of the southwest Taiwan fold-and-thrust belt occurs, then we can begin to investigate whether or not there is a causal relationship between this transverse zone and some aspects of the morphology and/or structure of the Eurasian margin. The *P* wave velocity model provides a key data set for investigating whether or not such a causal link exists, since it allows us to interpret features at depth below the fold-and-thrust belt that may be related to structures in the basement that are being inherited from the margin (Brown et al., 2017). For example, a 6-km depth slice through the *P* wave velocity model (Figure 10) shows a north-northeast trending velocity high through the study area that is bounded to the south by a north-northeast trending velocity low. These may be constituted by more than one velocity high and low, but, as stated in section 4, our tomography can only resolve minimum volumes of 20 km by 20 km by 10 km thick (Kuo-Chen et al., 2012). Nevertheless, this is well within the range to resolve basement highs and lows such as those imaged on the necking zone of the margin by reflection seismic and wide-angle tomography profiles (e.g., Brown et al., 2017; Lester et al., 2014; Li et al., 2007; McIntosh et al., 2014). We therefore interpret the velocity high and low in Figure 10 to be related to a basement high (Tainan Basement High) and low (Kaoshiung Basement Low).

By mapping the contours of the basal thrust derived from our 3-D structural model on the 6 km Vp depth slice (Figure 10), it is evident that, even given the resolution of the velocity model, there is good correlation between the location of the Yichu and Hsinhua oblique ramps and the Tainan Basement High. Furthermore, this correlation suggests that the topography of the basement has a roughly northeast to east-northeast striking structural grain, similar to that of extensional fault systems mapped on the margin offshore (e.g., A. T. Lin et al., 2003; Yang et al., 1991, 2016). On the basis of this correlation we suggest that it is possible to interpret a causative link between structures in the fold-and-thrust belt (i.e., oblique ramps and transverse zones) and features that are inherited from the continental margin (basement highs and lows). While we draw smooth, continuous contours for the basal thrust, it is likely that the east-northeast striking faults that bound similar basement highs and lows offshore, and which extend into the Coastal Plain (e.g., S. T. Huang et al., 2004; A. T. Lin et al., 2003; Yang et al., 1991, 2016), also bound the Tainan Basement High. The widespread occurrence of seismicity below the basal thrust and with dextral strike-slip focal mechanisms in the area around the Tainan Basement High (e.g., Hsu et al., 2010; Wu et al., 2010) is, furthermore, suggestive of reactivation of these faults. Since these reactivating faults are active over the same geological time frame as the basal thrust, this will cause the basal thrust to accommodate to the reactivating fault via a lateral ramp and/or a breaching of the basal thrust, implying a complex kinematic and geometrical relationship between them (e.g., Bayona et al., 2003; Calassou et al., 1993; Thomas, 1990; Thomas & Bayona, 2002; Turner et al., 2010) that, we think, will result in the formation of structures such as those described for

Hsinhua transverse zone. Numerous authors (e.g., Alvarez-Marron et al., 2014; Brown et al., 2017; Mouthereau et al., 2001; Mouthereau & Lacombe, 2006; Rodriguez-Roa & Wiltschko, 2010; Suppe, 1986; Yang et al., 2007, 2016) interpret structural complexities in the geology of southwest Taiwan to be related to the reactivation of such faults, although it is not always clear from these interpretations how the interaction between the reactivated faults and the basal thrust is coupled (or not). An exception is Mouthereau and Lacombe (2006) who interpret an imbricate thrust system in which thrusts sole into a ductile shear zone at about 15-km depth. Regardless, widespread seismic activity throughout nearly the entire crust in southwest Taiwan (Chang et al., 2007; Chao et al., 2011; Hsu et al., 2010; Wu et al., 2010; Yang et al., 2016) suggests that both the preexisting faults of the margin and those of the fold-and-thrust belt are all currently active.

Following the interpretation of Brown et al. (2017), the study area corresponds structurally to the intensely faulted necking zone and the beginning of the hyperextended part of the margin and, morphologically, to the outer shelf, the shelf-to-slope transition, and the slope (Figures 1 and 4). In the above discussion, we have dealt with the possible causal relationships between structures inherited from the margin and those in the fold-and-thrust belt. In what follows, we briefly look at possible linkages between the morphological parts of the margin and the structure of the fold-and-thrust belt. In southwestern Taiwan, both the mapped surface trace of thrusts and the subsurface contours of the basal thrust undergo a series of sigmoidal bends to take on an orientation that approximates that of the shelf-slope break and the onset of the hyperextended part of the margin (Brown et al., 2017; Figures 4 and 10). It is at the shelf-slope break where the frontal thrust of the fold-and-thrust belt goes offshore to form the front of the marine accretionary prism (Figure 1; see also A. T. Lin et al., 2008). Furthermore, the area encompassed by the Yichu and Hsinhua oblique ramps roughly correlates in location and strike with a significant southeastward increase in thickness of the Miocene through Pleistocene sediments (e.g., Chou, 1972, 1980) and with a change in facies toward deeper water deposits (Castelltort et al., 2010; Chou, 1972; Lin & Watts, 2002; Nagel et al., 2013). Therefore, another factor that may be influencing the along-strike structural changes in the southwest Taiwan fold-and-thrust belt could be related to mechanical differences along the basal thrust (e.g., Albers, 1967; Koyi et al., 2016; Mugnier et al., 1999; Ruh et al., 2014) that can be caused by changes in sedimentary thickness and facies. Although Mouthereau et al. (2001) explore some aspects of the influence of stratigraphic thickness and facies on the structure of the fold-and-thrust belt, we feel that more work, which should include numerical modeling, needs to be carried out before we can begin to draw conclusions about the influence of changes in sedimentary thickness and facies on the fold-and-thrust belt in southwest Taiwan.

7. Conclusions

On the basis of our new surface geological mapping, we interpret the structure of the fold-and-thrust belt in southwest Taiwan to be an imbricate thrust system with a pronounced north-south change in structural architecture across a roughly east-west striking zone that we call the Hsinhua transverse zone. The Hsinhua transverse zone falls along the on land projection of the shelf-slope break (Figures 4 and 10), and it coincides with Zone C of Brown et al. (2017). In this interpretation, the northern part of the study area comprises five thrust sheets: the Changhua, Chelungpu, Chutochi, Pingshi, and Chishan thrust sheets, whereas to the south of the Hsinhua transverse zone we divide the structure broadly into Changhua thrust sheet, the Xuxian antiform, and the Kuanglin synform (Figure 5). In our balanced and restored cross sections, we interpret the tip line of the basal thrust to be the buried Changhua thrust and, in the west, to lie within the Pliocene or Pleistocene synorogenic sediments before ramping down stratigraphic section eastward into the Early and Middle Miocene rocks and finally into the basement along the Chishan thrust. We estimate the minimum shortening across the fold-and-thrust belt in southwest Taiwan to be on the order of 17 and 25 km.

Overall, the basal thrust to the imbricate thrust system dips gently southeastward, but it has two pronounced sigmoidal changes in strike that form what we call the Yichu and Hsinhua oblique ramps. We suggest that the dextral strike-slip faulting, sigmoidal bending of the surface trace of thrusts, folds axes, and bedding (i.e., the Hsinhua transverse zone), together with the along-strike change in structure that occur in the fold-and-thrust belt of southwest Taiwan can be directly linked to these two oblique ramps. We furthermore suggest that both these oblique ramps can be directly correlated with topographic highs and lows that we interpret to occur in the basement (Figure 10) and that this possibly indicates a causative relationship between the

basement structure, the geometry of the basal thrust, and the along-strike changes mapped in the surface geology. We also acknowledge that the along-strike structural changes in the southwest Taiwan fold-and-thrust belt could also, in part, be related to mechanical differences along the basal thrust that can be caused by the changes in sedimentary thickness and facies that take place across the outer part of the shelf and the slope areas of the margin.

Acknowledgments
D. B., J. A-M., and C. B. acknowledge funding provided by the Spanish Ministerio de Economia y Competividad grant CGL2013-43877-P. H. K-C. acknowledges funding by MOST 104-2628-M-008-005-MY3. Constructive reviews by C. von Hagke and an anonymous reviewer are also acknowledged. The geological data presented in this paper can be found in the supporting information in the form of a 1:100,000 scale map and a.txt file for the structural data. The seismic tomography data from which Figure 10 was plotted can be found at http://140.115.22.221/download/data.

References

Albers, J. P. (1967). Belt of sigmoidal bending and right-lateral faulting in the Western great Basin. *Geological Society of America Bulletin*, *78*(2), 143–156. https://doi.org/10.1130/0016-7606(1967)78[143:BOSBAR]2.0.CO;2

Alvarez-Marron, J. (1995). Three-dimensional geometry and interference of fault-bend fold: Examples from the Ponga Unit, Variscan Belt, NW Spain. *Journal of Structural Geology*, *17*(4), 549–560. https://doi.org/10.1016/0191-8141(94)00075-B

Alvarez-Marron, J., Brown, D., Camanni, G., Wu, Y.-M., & Kuo-Chen, H. (2014). Structural complexities in a foreland thrust belt inherited from the shelf-slope transition: Insights from the Alishan area of Taiwan. *Tectonics*, *33*, 1322–1339. https://doi.org/10.1002/2014TC003584.

Arora, B. R., Gahalaut, V. K., & Kumar, N. (2012). Structural control on along-strike variation in the seismicity of the northwest Himalaya. *Journal of Asian Earth Sciences*, *57*, 15–24. https://doi.org/10.1016/j.jseaes.2012.06.001

Bayona, G., Thomas, W. A., & Van der Voo, R. (2003). Kinematics of thrust sheets within transverse zones: A structural and paleomagnetic investigation in the Appalachian thrust belt of Georgia and Alabama. *Journal of Structural Geology*, *25*(8), 1193–1212. https://doi.org/10.1016/S0191-8141(02)00162-1

Bonilla, M. G. (1975). A review of recently active faults in Taiwan, USGS Open-File Rep. 75-41, 43.

Boyer, S. E., & Elliott, D. (1982). Thrust systems. *American Association of Petroleum Geologists*, *66*, 1196–1230.

Brown, D., Alvarez-Marron, J., Biete, C., Kuo-Chen, H., Camanni, G., & Ho, C.-W. (2017). How the structural architecture of the Eurasian continental margin affects the structure, seismicity, and topography of the south central Taiwan fold-and-thrust belt. *Tectonics*, *36*, 1275–1294. https://doi.org/10.1002/2017TC004475

Brown, D., Alvarez-Marron, J., Schimmel, M., Wu, Y.-M., & Camanni, G. (2012). The structure and kinematics of the central Taiwan mountain belt derived from geological and seismicity data. *Tectonics*, *31*, TC5013. https://doi.org/10.1029/2012TC003156

Butler, R. W. H., Tavarnelli, E., & Grasso, M. (2006). Structural inheritance in mountain belts: An Alpine–Apennine perspective. *Journal of Structural Geology*, *28*(11), 1893–1908. https://doi.org/10.1016/j.jsg.2006.09.006

Calassou, S., Larroque, C., & Malavieille, J. (1993). Transfer zones of deformation in thrust wedges: An experimental study. *Tectonophysics*, *221*(3-4), 325–344. https://doi.org/10.1016/0040-1951(93)90165-G

Camanni, G., Alvarez-Marron, J., Brown, D., Ayala, C., Wu, Y.-M., & Hsieh, H.-H. (2016). The deep structure of south-central Taiwan illuminated by seismic tomography and earthquake hypocentre data. *Tectonophysics*, *679*, 235–245. https://doi.org/10.1016/j.tecto.2015.09.016

Castelltort, S., Nagel, S., Moutherreau, F., Lin, A., Wetzel, A., Kaus, B., et al. (2010). Sedimentology of Early Pliocene sandstones in the southwestern Taiwan foreland: Implications for basin physiography in the early stages of collision. *Journal of Asian Earth Sciences*, *40*, 52–71.

Chang, S. (1963). Regional stratigraphic study of Pleistocene and upper Pliocene formations in Chiayi and Hsinying area. *Petroleum Geology of Taiwan*, *2*, 65–85.

Chang, C.-H., Wu, Y.-M., Zhao, L., & Wu, F. T. (2007). Aftershocks of the 1999 Chi-Chi, Taiwan, Earthquake: The first hour. *Bulletin of the Seismological Society of America*, *97*(4), 1245–1258. https://doi.org/10.1785/0120060184

Chao, W.-A., Zhao, L., & Wu, Y.-M. (2011). Centroid fault-plane inversion in three-dimensional velocity structure using strong-motion records. *Bulletin of the Seismological Society of America*, *101*(3), 1330–1340. https://doi.org/10.1785/0120100245

Chen, C.-H., Ho, H.-C., Shea, K.-S., Lo, W., Lin, W.-H., Chang, H.-C., et al. (2000). Geological map of Taiwan. 1:500,000 scale, Central Geol. Sur., Taiwan.

Chen, W.-S., Ridgway, K. D., Horng, C.-S., Chen, Y.-G., Shea, K.-S., & Yeh, M.-G. (2001). Stratigraphic architecture, magnetostratigraphy, and incised-valley systems of the Pliocene-Pliestocene collisional marine foreland basin of Taiwan. *Geological Society of America Bulletin*, *113*(10), 1249–1271. https://doi.org/10.1130/0016-7606(2001)113<1249:SAMAIV>2.0.CO;2

Chiang, S. C. (1971). Seismic study of the Paishatun structure, Miaoli, Taiwan. *Petroleum Geology of Taiwan*, *8*(8), 281–294.

Chiang, C., Yuw, H., & Chouz, Y. (2004). Characteristics of the wedge-top depozone of the southern Taiwan foreland basin system. *Basin Research*, *16*(1), 65–78. https://doi.org/10.1111/j.1365-2117.2003.00222.x

Ching, K.-E., Rau, R.-J., Johnson, K. M., Lee, J.-C., & Hu, J.-C. (2011). Present-day kinematics of active mountain building in Taiwan from GPS observations during 1995-2005. *Journal of Geophysical Research*, *116*, B09405. https://doi.org/10.1029/2010JB008058

Chiu, H. T. (1975). Miocene stratigraphy and its relation to the Palaeogene rocks in West - Central Taiwan. *Petroleum Geology of Taiwan*, *12*, 51–80.

Chou, J. T. (1971). A preliminary study of the stratigraphy and sedimentation of the mudstone formations in the Tainan area, southern Taiwan. *Petroleum Geology of Taiwan*, *8*, 187–220.

Chou, J. T. (1972). A sedimentologic and paleogeographic study of the upper Cenozoic clastic sequences in the Chiayi region, Western Taiwan. *Petroleum Geology of Taiwan*, *10*, 141–158.

Chou, J. T. (1980). Stratigraphy and sedimentology of the Miocene in western Taiwan. *Petroleum Geology of Taiwan*, *17*, 33–52.

Covey, M. (1986). The evolution of foreland basins to steady state: Evidence from the western Taiwan Foreland Basin. In *Foreland Basins* (pp. 77–90). Oxford, UK: Blackwell Publishing Ltd. https://doi.org/10.1002/9781444303810.ch4

Dahlstrom, C. D. A. (1969). Balanced cross sections. *Canadian Journal of Earth Sciences*, *6*(4), 743–757. https://doi.org/10.1139/e69-069

De Paor, D. G. (1988). Balanced section in thrust belts part 1: Construction. *American Association of Petroleum Geologists Bulletin*, *72*, 73–90.

Deffontaines, B., Lacombe, O., Angelier, J., Chu, H.-T., Mouthereau, F., Lee, C.-T., et al. (1997). Quaternary transfer faulting in the Taiwan Foorhills: Evidence from a multisource approach. *Tectonophysics*, *274*(1-3), 61–82. https://doi.org/10.1016/S0040-1951(96)00298-3

Ding, W.-W., Li, J.-B., Li, M.-B., Qiu, X.-L., Fang, Y.-X., & Tang, Y. (2008). A Cenozoic tectono-sedimentary model of the Tainan Basin, the South China Sea: Evidence from multi-channel seismic profile. *Journal of Zhejiang University. Science*, *9*(5), 702–713. https://doi.org/10.1631/jzus.A071572

Duncan, C., Masek, J., & Fielding, E. (2003). How steep are the Himalaya? Characteristics and implications of along-strike topographic variations. *Geology*, *31*(1), 75–78. https://doi.org/10.1130/0091-7613(2003)031<0075:HSATHC>2.0.CO;2

Elliott, D., & Johnson, M. R. W. (1980). Structural evolution in the northern part of the Moince thrust belt, NW Scotland. *Transactions of the Royal Society of Edinburgh Earth Sciences*, *71*(02), 69–96. https://doi.org/10.1017/S0263593300013523

Ernst, W. G. (1983). Mineral paragenesis in metamorphic rocks exposed along Tailuko Gorge, Central Mountain Range, Taiwan. *Journal of Metamorphic Geology*, *1*(4), 305–329. https://doi.org/10.1111/j.1525-1314.1983.tb00277.x

Faulds, J. E., & Varga, R. J. (1998). The role of accommodation zones and transfer zones in the regional segmentation of extended terranes. In J. E. Faulds & J. H. Stewart (Eds.), *Accommodation zones and transfer zones: The regional segmentation of the basin and range province*, *Geol. Soc. Am. Spec. Paper* (Vol. 323, pp. 1–45). Boulder, CO.

Flöttmann, T., & James, P. (1997). Influence of basin architecture on the style of inversion and fold-thrust belt tectonics—The southern Adelaide fold-thrust belt, South Australia. *Journal of Structural Geology*, *19*(8), 1093–1110. https://doi.org/10.1016/S0191-8141(97)00033-3

Groshong, R. H., Bond, C. E., Gibbs, A., Ratliff, R., & Wiltschko, D. V. (2012). Preface: Structural balancing at the start of the 21st century: 100 years since Chamberlin. *Journal of Structural Geology*, *41*, 1–5. https://doi.org/10.1016/j.jsg.2012.03.010

Ho, C. S. (1986). A synthesis of the geologic evolution of Taiwan. *Tectonophysics*, *125*(1-3), 1–16. https://doi.org/10.1016/0040-1951(86)90004-1

Ho, C.-S. (1988). An Introduction to the Geology of Taiwan: Explanatory text of the Geological Map of Taiwan, Central Geological Survey. Taipei, Taiwan.

Hong, E. (1997). Evolution of Pliocene to Pleistocene sedimentary environments in an arc-continent collision zone: Evidence from the analyses of lithofacies and ichnofacies in the southwestern foothills of Taiwan. *Journal of Asian Earth Sciences*, *15*(4–5), 381–392. https://doi.org/10.1016/S0743-9547(97)00022-6

Horng, C. S., & Shea, K.-S. (1994). Study of nannofossil biostratigraphy in the eastern part of the Erhjen-chi section, southwestern Taiwan. *Special Publication of Centre Geological Survey*, *8*, 181–204.

Horng, C.-S. (2014). Age odd the Tananwan Formation in northern Taiwan: A reexamination of the magnetostratigraphy and calcareous nannofossil biostratigraphy. *Terrestrial, Atmospheric and Oceanic Sciences*, *25*, 137–147.

Hossack, J. R. (1979). The use of balanced cross-sections in the calculation of orogenic contraction: A review. *Journal of the Geological Society*, *136*(6), 705–711. https://doi.org/10.1144/gsjgs.136.6.0705

Hossack, J. R. (1983). A cross-section through the Scandinavian Caledonides constructed with the aid of branch-line maps. *Journal of Structural Geology*, *5*(2), 103–111. https://doi.org/10.1016/0191-8141(83)90036-6

Hsu, Y.-J., Rivera, L., Wu, Y.-M., Chang, C.-H., & Kanamori, H. (2010). Spatial heterogeneity of tectonic stress and friction in the crust: New evidence from earthquake focal mechanisms in Taiwan. *Geophysical Journal International*, *182*, 329–342.

Huang, M.-H., Hu, J.-C., Ching, K.-E., Rau, R.-J., Hsieh, C.-S., Pathier, E., et al. (2009). Active deformation of Tainan tableland os southwestern Taiwan based on geodetic measurements and SAR interferometry. *Tectonophysics*, *466*(3-4), 322–334. https://doi.org/10.1016/j.tecto.2007.11.020

Huang, C. Y., Yen, Y., Zhao, Q. H., & Lin, C. T. (2012). Cenozoic stratigraphy of Taiwan: Window into rifting, stratigraphy and paleoceanography of South China Sea. *Chinese Science Bulletin*, *57*(24), 3130–3149. https://doi.org/10.1007/s11434-012-5349-y

Huang, L.-S. (1984). Iodine contents in formation waters from wildcats, southern Taiwan. *Petroleum Geology of Taiwan*, *20*, 215–235.

Huang, S. T., Yang, K.-M., Hung, J.-H., Wu, J. C., Ting, H. H., Mei, W. W., et al. (2004). Deformation front development at the northeast margin of the Tainan basin, Tainan-Kaohsiung area, Taiwan. *Marine Geophysical Researches*, *25*(1–2), 139–156. https://doi.org/10.1007/s11001-005-0739-z

Jahn, B.-M., Chi, W.-R., & Yui, T.-F. (1992). A Late Permian formation of Taiwan marbles from Chia-Li well No.1: Pb-Pb isochron and Sr isotopic evidence, and its regional geological significance. *Journal of the Geological Society of China*, *35*, 193–218.

Judge, P. A., & Allmendinger, R. W. (2011). Assessing uncertainties in balanced cross sections. *Journal of Structural Geology*, *33*, 458–467.

Koyi, H., Nilfouroushan, F., & Hessami, K. (2016). Modelling role of basement block rotation and strike-slip faulting on structural pattern in cover units of fold-and-thrust belts. *Geological Magazine*, *153*(5-6), 827–844. https://doi.org/10.1017/S0016756816000595

Kuo-Chen, H., Wu, F. T., & Roecker, S. W. (2012). Three-dimensional P velocity structures of the lithosphere beneath Taiwan from the analysis of TAIGER and related seismic data sets. *Journal of Geophysical Research*, *117*, B06306. https://doi.org/10.1029/2011JB009108

Lacombe, O., Mouthereau, F., Angelier, J., & Deffontaines, B. (2001). Structural, geodetic and seismological evidence for tectonic escape in SW Taiwan. *Tectonophysics*, *333*(1-2), 323–345. https://doi.org/10.1016/S0040-1951(00)00281-X

Lacombe, O., Mouthereau, F., Deffontaines, B., Angelier, J., Chu, H. T., & Lee, C. T. (1999). Geometry and Quaternary kinematics of fold-and-thrust units of southwestern Taiwan. *Tectonics*, *18*(6), 1198–1223. https://doi.org/10.1029/1999TC900036

Lan, C.-Y., Lee, C.-S., Yui, T.-F., Chu, H.-T., & Jahn, B.-M. (2008). The tectono-thermal events of Taiwan and their relationship with SE China. *Terrestrial, Atmospheric and Oceanic Sciences*, *19*(3), 257–278. https://doi.org/10.3319/TAO.2008.19.3.257(TT)

Lee, T.-Y., Tang, C.-H., Ting, J.-S., & Hsu, Y.-Y. (1993). Sequence stratigraphy of the Tainan Basin, offshore Southwestern Taiwan. *Petroleum Geology of Taiwan*, *28*, 119–158.

Lester, R., Van Avendonk, H. J. A., McIntosh, K., Lavier, L., Liu, C.-S., Wang, T.-K., & Wu, F. (2014). Rifting and magmatism in the northeastern South China Sea from wide-angle tomography and seismic reflection imaging. *Journal of Geophysical Research: Solid Earth*, *119*, 2305–2323. https://doi.org/10.1002/2013JB010639

Li, C.-F., Zhou, Z., Li, J., Hao, H., & Geng, J. (2007). Structures of the northeasternmost South China Sea continental margin and ocean basin: Geophysical constraints and tectonic implications. *Marine Geophysical Researches*, *28*(1), 59–79. https://doi.org/10.1007/s11001-007-9014-9

Lin, A. T., Liu, C.-S., Lin, C. C., Schnurle, P., Chen, G. Y., Liao, W. Z., et al. (2008). Tectonic features associated with the overriding of an accretionary wedge on top of a rifted continental margin: An example from Taiwan. *Marine Geology*, *255*(3–4), 186–203. https://doi.org/10.1016/j.margeo.2008.10.002

Lin, A. T., & Watts, A. B. (2002). Origin of the West Taiwan basin by orogenic loading and flexure of a rifted continental margin. *Journal of Geophysical Research*, *107*(B9), 2185. https://doi.org/10.1029/2001JB000669

Lin, A. T., Watts, A. B., & Hesselbo, S. P. (2003). Cenozoic stratigraphy and subsidence history of the South China Sea margin in the Taiwan region. *Basin Research*, *15*(4), 453–478. https://doi.org/10.1046/j.1365-2117.2003.00215.x

Lin, J.-Y., Sibuet, J.-C., & Hsu, S.-K. (2005). Distribution of the East China Sea continental shelf basins and depths of magnetic sources. *Earth, Planets and Space*, *57*(11), 1063–1072. https://doi.org/10.1186/BF03351885

McIntosh, K., Lavier, L., Van Avendonk, H., Lester, R., Eakin, D., & Liu, C.-S. (2014). Crustal structure and inferred rifting processes in the northeast South China Sea. *Marine and Petroleum Geology*, *58*, 612–626. https://doi.org/10.1016/j.marpetgeo.2014.03.012

Mouthereau, F., Deffontaines, B., Lacombe, O., & Angelier, J. (2002). Variations along the strike of the Taiwan thrust belt: Basement control on structural style, wedge geometry, and kinematics. In T. B. Byrne & C.-S. Liu (Eds.), *Geology and geophysics of an arc-continent collision, Taiwan*, *Geol. Soc. am. Spec. Paper* (Vol. 358, pp. 31–54).

Mouthereau, F., & Lacombe, O. (2006). Inversion of the Paleogene Chinese continental margin and thick-skinned deformation in the Western Foreland of Taiwan. *Journal of Structural Geology*, *28*(11), 1977–1993. https://doi.org/10.1016/j.jsg.2006.08.007

Mouthereau, F., Lacombe, O., Deffontaines, B., Angelier, J., & Brusset, S. (2001). Deformation history of the southwestern Taiwan foreland thrust belt: Insights from tectono-sedimentary analyses and balanced cross-sections. *Tectonophysics*, *333*(1–2), 293–322. https://doi.org/10.1016/S0040-1951(00)00280-8

Mouthereau, F., Lacombe, O., Deffontaines, B., Angelier, J., Chu, H.-T., & Lee, C.-T. (1999). Quaternary transfer faulting and belt front deformation at Pakuashan (western Taiwan). *Tectonics*, *18*(2), 215–230. https://doi.org/10.1029/1998TC900025

Mouthereau, F., Lacombe, O., & Meyer, B. (2006). The Zagros folded belt (Fars, Iran): Constraints from topography and critical wedge modeling. *Geophysical Journal International*, *165*, 336–356.

Mugnier, J. L., Leturmy, P., Mascle, G., Huyghe, P., Chalaron, E., Vidal, G., et al. (1999). The Siwaliks of western Nepal I. Geometry and kinematics. *Journal of Asian Earth Sciences*, *17*(5-6), 629–642. https://doi.org/10.1016/S1367-9120(99)00038-3

Nagel, S., Castelltort, S., Wetzel, A., Willett, S. D., Mouthereau, F., & Lin, A. T. (2013). Sedimentology and foreland basin paleogeography during Taiwan arc continent collision. *Journal of Asian Earth Sciences*, *62*, 180–204. https://doi.org/10.1016/j.jseaes.2012.09.001

Oncken, O., von Winterfeld, C., & Dittmar, U. (1999). Accretion of a rifted passive margin: The Late Paleozoic Rhenohercynian fold and thrust belt (Middle European Variscides). *Tectonics*, *18*(1), 75–91. https://doi.org/10.1029/98TC02763

Pérez-Estaún, A., Alvarez-Marrón, J., Brown, D., Puchkov, V., Gorozhanina, Y., & Baryshev, V. (1997). Along-strike structural variations in the foreland thrust and fold belt of the southern Urals. *Tectonophysics*, *276*(1-4), 265–280. https://doi.org/10.1016/S0040-1951(97)00060-7

Rodriguez-Roa, F. a., & Wiltschko, D. V. (2010). Thrust belt architecture of the central and southern Western Foothills of Taiwan. *Geological Society of London, Special Publication*, *348*(1), 137–168. https://doi.org/10.1144/SP348.8

Ruh, J. B., Gerya, T., & Burg, J.-P. (2014). 3D effects of strain vs. velocity weakening on deformation patterns in accretionary wedges. *Tectonophysics*, *615-616*, 122–141. https://doi.org/10.1016/j.tecto.2014.01.003

Shaw, C.-L. (1996). Stratigraphic correlation and isopach maps of the western Taiwan Basin. *Terrestrial, Atmospheric and Oceanic Sciences*, *7*(3), 333–360. https://doi.org/10.3319/TAO.1996.7.3.333(T)

Shea, K.-S., Chang, H.-C., Huang, T.-Y., Ho, H.-C., Lin, W.-H., Lin, C.-W., & Chen, H.-W. (2003). Geological Column in Taiwan, *Central Geol. Surv. Taiwan*, Taiwan.

Shi, X., Xu, H., Qiu, X., Xia, K., Yang, X., & Li, Y. (2008). Numerical modeling on the relationship between thermal uplift and subsequent rapid subsidence: Discussion on the evolution of the Tainan Basin. *Tectonics*, *27*, TC6003. https://doi.org/10.1029/2007TC002163

Shyu, J. B. H., Chuang, Y., Chen, Y., Lee, Y., & Cheng, C. (2016). A new on-land seismogenic structure source database from the Taiwan earthquake model (TEM) project for seismic hazard analysis of Taiwan. *Terrestrial, Atmospheric and Oceanic Sciences*, *27*(3), 311–323. https://doi.org/10.3319/TAO.2015.11.27.02(TEM)A

Shyu, J. B. H., Sieh, K., Chen, Y.-G., & Liu, C.-S. (2005). Neotectonic architecture of Taiwan and its implications for future large earthquakes. *Journal of Geophysical Research*, *110*, B08402. https://doi.org/10.1029/2004JB003251

Smith, N. T. (1999). Variscan inversion within the Cheshire Basin, England: Carboniferous evolution north of the Variscan Front. *Tectonophysics*, *308*, 211–225.

Srivastava, P., & Mitra, G. (1994). Thrust geometries and deep structure of the outer and lesser Himalaya, Kumaon and Garhwal (India): Implications for the evolution of the Himalayan fold-and-thrust belt. *Tectonics*, *13*(1), 89–109. https://doi.org/10.1029/93TC01130

Stanley, R. S., Hill, L. B., Chang, H. C., & Hu, H. N. (1981). A transect through the metamorphic core of the central mountains, southern Taiwan. *Memoir of Geological Society of China*, *4*, 443–473.

Suppe, J. (1981). Mechanics of mountain-building and metamorphism in Taiwan. *Memoir of Geological Society of China*, *4*, 67–89.

Suppe, J. (1986). Reactivated normal faults in the western Taiwan fold-and-thrust belt. *Memoir of Geological Society of China*, *7*, 187–200.

Tang, C.-H. (1977). Late Miocene erosional unconformity on the subsurface Peikang high Chiayi Yulin. *Memoir of Geological Society of China*, *2*, 155–167.

Tang, Q., & Zheng, C. (2010). Seismic velocity structure and improved seismic image of the Southern Depression of the Tainan Basin from pre-stack depth migration. *Terrestrial, Atmospheric and Oceanic Sciences*, *21*(5), 807–816. https://doi.org/10.3319/TAO.2010.01.03.01(TT)

Teng, L.-S. (1987). Stratigraphic records of the Late Cenozoic Penglai Orogeny of Taiwan. *Acta Geologica Taiwanica*, *25*, 205–224.

Teng, L.-S., & Lin, A.-T. (2004). Cenozoic tectonics of the China continental margin: Insights from Taiwan. In J. Malpas, C. J. N. Fletcher, J. R. Ali, & J. C. Aitchison (Eds.), *Aspects of the tectonic evolution of China*, *Geol. Soc. London, Spec. Pub.* (Vol. 226, pp. 313–332). Geological Society, London.

Tensi, J., Mouthereau, F., & Lacombe, O. (2006). Lithospheric bulge in the West Taiwan Basin. *Basin Research*, *18*(3), 277–299. https://doi.org/10.1111/j.1365-2117.2006.00296.x

Thomas, W. A. (1985). The Appalachian-Ouachita connection: Paleozoic orogenic belt at the southern margin of North America. *Annual Review of Earth and Planetary Sciences*, *13*(1), 175–199. https://doi.org/10.1146/annurev.ea.13.050185.001135

Thomas, W. A. (1990). Controls on locations of transverse zones in thrust belts. *Eclogae Geologicae Helvetiae*, *83*, 727–744.

Thomas, W. A., & Bayona, G. (2002). Palinspastic restoration of the Anniston transverse zone in the Appalachian thrust belt, Alabama. *Journal of Structural Geology*, *24*(4), 797–826. https://doi.org/10.1016/S0191-8141(01)00117-1

Turner, S. A., Cosgrove, J. W., & Liu, J. G. (2010). Controls on lateral structural variability along the Keping Shan Thrust Belt, SW Tien Shan foreland, China. In G. P. Goffey, J. Craig, T. Needham, & R. Scott (Eds.), *Hydrocarbons in contractional belts*, *Geological Society of London, Special Publications* (Vol. 348, pp. 71–85). Geological Society, London. https://doi.org/10.1144/SP348.5

Woodward, N. B. (1986). Thrust fault geometry of the Snake River Range, Idaho and Wyoming. *Geological Society of America Bulletin*, *97*(2), 178–193. https://doi.org/10.1130/0016-7606(1986)97<178:TFGOTS>2.0.CO;2

Wu, Y.-M., Hsu, Y.-J., Chang, C.-H., Teng, L. S.-Y., & Nakamura, M. (2010). Temporal and spatial variation of stress in Taiwan from 1991 to 2007: Insights from compressive first motion focal mechanism catalog. *Earth and Planetary Science Letters*, *298*(3-4), 306–316. https://doi.org/10.1016/j.epsl.2010.07.047

Yang, K.-M., Huang, S. T., Wu, J.-C., Ting, H.-H., & Mei, W.-W. (2006). Review and new insights on foreland tectonics in western Taiwan. *International Geology Review*, *48*(10), 910–941. https://doi.org/10.2747/0020-6814.48.10.910

Yang, K.-M., Huang, S.-T., Wu, J.-C., Ting, H.-H., Mei, W.-W., Lee, M., et al. (2007). 3D geometry of the Chelungpu thrust system in Central Taiwan: Its implications for active tectonics. *Terrestrial, Atmospheric and Oceanic Sciences*, *18*, 143–181.

Yang, K.-M., Rau, R.-J., Chang, H.-Y., Hseih, C.-Y., Ting, H.-H., Huang, S.-T., et al. (2016). The role of basement-involved normal faults in the recent tectonics of western Taiwan. *Geological Magazine*, *153*(5-6), 1166–1191. https://doi.org/10.1017/S0016756816000637

Yang, K.-M., Ting, H.-H., & Yuan, J. (1991). Structural styles and tectonic modes of Neogene extensional tectonics in southwestern Taiwan: Implications for hydrocarbon exploration. *Petroleum Geology of Taiwan*, *26*, 31.

Yang, K.-M., Wu, J.-C., Cheng, E.-W., Chen, Y.-R., Huang, W.-C., Tsai, C.-C., et al. (2014). Development of tectonostratigraphy in distal part of foreland basin in southwestern Taiwan. *Journal of Asian Earth Sciences*, *88*, 98–115. https://doi.org/10.1016/j.jseaes.2014.03.005

Yin, A. (2006). Cenozoic tectonic evolution of the Himalayan orogeny as constrained by along-strike variation of structural geometry, exhumation history, and foreland sedimentation. *Earth Science Reviews*, *76*(1-2), 1–131. https://doi.org/10.1016/j.earscirev.2005.05.004

Yu, S., Chen, H., & Kuo, L. (1997). Velocity field of GPS stations in the Taiwan area. *Tectonophysics*, *274*(1-3), 41–59. https://doi.org/10.1016/S0040-1951(96)00297-1

Yuan, J., & Huang, S. T. (1985). Stratigraphic study on the pre Miocene under the Peikang Area.

Zanchi, A., Berra, F., Mattei, M., Ghassemi, M. R., & Sabouri, J. (2006). Inversion tectonics in the central Alboraz, Iran. *Journal of Structural Geology*, *28*(11), 2023–2037. https://doi.org/10.1016/j.jsg.2006.06.020